



Bajocian–Bathonian dinoflagellate cyst assemblages from the Middle Atlas, Morocco: Palynostratigraphic and paleoenvironmental implications



Hanane Khaffou ^a, Touria Hssaida ^a, Mostafa Oukassou ^{b,*}, Wafaa Maatouf ^c, Abdelkrim Afenzar ^d, Omar Zafaty ^b, Sara Chakir ^d, Soukaina Jaydawi ^e, Khaoula Chafai ^a, André Charrière ^f

^a Geosciences and Applications Laboratory, Faculty of Sciences Ben M'sick, Hassan II University of Casablanca, Casablanca, Morocco

^b Applied Geology, Geoinformatics and Environment Laboratory, Faculty of Sciences Ben M'sick, Hassan II University of Casablanca, Casablanca, Morocco

^c Department of Petroleum Laboratory, National Office of Hydrocarbons and Mining (ONHYM), Rabat, Morocco

^d Geosciences, Environment and Associated Resources Laboratory, Faculty of Sciences Dhar El Mahraz, Sidi Mohamed Ben Abdellah University, Fes, Morocco

^e Mohammed V University, Faculty of Sciences, Rabat, Morocco

^f Toulouse III University, Anduze, France

ARTICLE INFO

Article history:

Received 12 September 2022

Received in revised form 8 February 2023

Accepted 10 February 2023

Available online 16 February 2023

Keywords:

Biostratigraphy

Palynology

Dinoflagellate cysts

Bajocian–Bathonian

Middle Atlas

Morocco

ABSTRACT

The Bajocian–Bathonian transition has been identified for the first time in the Skoura syncline of the folded Middle Atlas of Morocco based on dinoflagellate cyst and palynofacies analysis of the Ich Timellaline/Bou Akrabene Formation carbonates. This palynological study involved 109 samples of marls and limestones whose organic content yielded diverse and well-preserved dinoflagellate cyst assemblages comprising 68 taxa including stratigraphic marker taxa. Two association biozones have been defined for the late Bajocian–early Bathonian interval. The *Cribroperidinium crispum*-*Ctenidodinium cornigerum* (CC/CC) biozone is defined between the base of the Recifa Formation (Upper Bajocian) and the Ich-Timellaline / Bou Akrabene Formation (Upper Bajocian–Lower Bathonian). The second association biozone of *Ctenidodinium combazii* and *Dichadogonyaulax sellwoodii* (CC/DS) corresponds to the upper interval of the FD section (top of the Ich-Timellaline / Bou Akrabene Formation and the base of the El Mers I Formation). These two biozones were correlated with the late Bajocian–early Bathonian biozones defined in the Sub-Boreal (northwest Europe), Tethyan, and Australian domains. Close similarity between the Moroccan Middle Atlas, the Tethyan, and the Sub-Boreal domain associations has been noted. Quantitative analysis of organic matter constituents has allowed the paleoenvironmental reconstruction of the late Bajocian–early Bathonian. The organic residues of the studied samples recorded an increased land-derived phytoplasm dominance compared to amorphous organic matter and palynomorphs, indicating a proximal oxic shelf depositional environment with high terrestrial and freshwater influx during the late Bajocian–early Bathonian. During the Late Bajocian, the depositional environment corresponds to a proximal continental shelf with fluctuations from a distal to a marginal/stagnant environment.

Below the Upper Bajocian–Lower Bathonian boundary, a significant marine incursion, or rather a transgression, is recorded in the studied sediments attested by an important marine fraction and dinoflagellate cysts abundance, which probably corresponds to the last Bajocian Maximum flooding surface (MFS).

During the early Bathonian, the depositional environment evolved towards a distal continental shelf with an increasing marine fraction including dinoflagellate cysts and high species diversity. This may be related to the rising sea level which corresponds to the first Bathonian eustatic elevation. The proximal /marginal conditions are restored at the uppermost part of the section.

© 2023 Elsevier B.V. All rights reserved.

1. Introduction

The Middle Atlas of Morocco is an intracontinental fold-thrust belt extending along the foreland of the Rif orogen. The stratigraphy of the Middle Atlas is essentially made up of Meso-cenozoic rocks. The Early and Middle Jurassic Tethyan marine successions crop out extensively

* Corresponding author.

E-mail address: mostafa.oukassou@univh2c.ma (M. Oukassou).

in this region. The earliest stratigraphic works were by [Colo \(1961\)](#) and [Dresnay \(1963\)](#), they used ammonites to date the late Bajocian–early Bathonian successively; The Dogger brachiopods in the Middle Atlas deposits have been first reported by [Rousselle \(1965, 1966\)](#). [Mongin \(1963, 1967\)](#) proposed the Bathonian–Callovian age by giving some insight into lamellibranch and gasteropod biostratigraphic distribution. The Bathonian was dated later by [Termier and Termier \(1967\)](#) using lamellibranchs. In 1969, [Dresnay](#) documented the presence of a “sub-cretaceous unconformity” separating the lower part of the Jurassic red beds from an upper part belonging to the Cretaceous. In the last decades of the twentieth century, [Charrière \(1989, 1990\)](#) studied the reds beds deposits in the Skoura syncline, and clearly separated the red beds of the Middle Jurassic (Bathonian–? Callovian) from those of the Lower Cretaceous (Barremian–Aptian) ([Charrière, 1992](#); [Charrière et al., 1994](#)) from the central Middle Atlas. In the El Mers syncline, [Fedan, \(1993\)](#) reported the presence of an ammonite specifying the age of El Mers 1 Formation from the folded Middle Atlas. More recently, [Charrière and Haddoumi \(2016\)](#) established a synthesis on Jurassic deposits. They discussed the sedimentology, the stratigraphy, the paleontology and the paleoenvironment of the continental red beds in Atlasic domains.

Several palynological studies on the Middle Jurassic (Dogger) have been carried out in several areas of the Tethyan realm. Nevertheless, the Middle Atlas palynological studies, dealing with the biostratigraphy of dinoflagellate cysts and paleoenvironment across the Bajocian–Bathonian interval are absent. In this work, we present the first palynological study based on dinoflagellate cysts biostratigraphy of the Middle Jurassic in this Atlasic domain of Morocco. Our study is carried out in the northwestern part of the Skoura syncline (Middle Atlas) through the Ich Timellaline-Bou Akrabene Formation. This palynological study may be a major contribution to the southwestern Tethyan margin background. The aims of this contribution are (*i*) to date this particular formation, and to define the Bajocian–Bathonian boundary based on dinoflagellate cyst distributions, (*ii*) to explore paleo-environmental trends using palynological association and palynofacies data, and (*iii*) to compare the distribution of dinoflagellate cyst taxa from this area with other localities in the world (North Tethyan, Boreal and Austral realms).

2. Geological setting

The Middle Atlas is a northeast-southwest trending mountain range extending between the western-Central Moroccan Meseta in the West and the High Moulouya and High Plateaus in the East ([Fig. 1A](#)). The Middle Atlas belongs to the Atlas system of intracontinental belts erected through the Alpine inversion of the Triassic–Early Jurassic rifts at the northern margin of the African plate ([Frizon de Lamotte et al., 2008](#)). The belt is characterized by NE–SW trending faults inherited from the major structures of the Variscan basement ([Charrière, 1990](#)). The Northern Middle Atlas Fault (NMAF) separates the faulted tabular Middle Atlas in the NW and the folded Middle Atlas in the SE ([Choubert, 1956](#); [Martin, 1973, 1981](#)). The latter consists of narrow anticlinal ridges associated with longitudinal faults and extrusions of Triassic tholeiitic basalts and evaporites, which are separated by wide and open synclines ([Colo, 1961](#)). The synsedimentary activity of these faulted ridges during the Jurassic has been repeatedly demonstrated ([Duée et al., 1977](#); [Fedan et al., 1989](#); [Laville and Fedan, 1989](#); [Charrière, 1990](#); [Fedan, 1993](#); [Scheele, 1994](#); [Rhrib, 1997](#)).

Located in the central part of the folded Middle Atlas, between the NMAF and the Tichoukt anticline ridge, the Skoura syncline exposes marine formations ranging from the lower to middle Jurassic followed by a thick regressive middle Jurassic deltaic and lagoonal sequences ([Dresnay, 1963, 1969, 1975](#); [Benshili, 1989](#); [Charrière, 1992](#); [Fedan, 1993](#); [Charrière et al., 1994](#); [Oukassou, 2018](#); [Oukassou et al., 2016, 2019](#)). These sequences are locally capped unconformably by the Wealdian? fluvial deposits ([Charrière and Haddoumi, 2016](#)). The strata exhibit a gentle dip on the northwestern flank of the syncline, whereas

they are vertical or even overturned on the southeastern flank underlying the Jebel Tichoukt transverse fault ([Fig. 1C](#)).

The studied section is located on the western flank of the Skoura syncline and is comprised between two transverse faults. This section extends through three Middle Jurassic lithological formations (Upper Bajocian –?Callovian) defined by [Dresnay \(1963\)](#) and [Charrière \(1989\)](#) ([Figs. 1C and 2](#)):

Recifa Formation or “Calcaire corniche” ([Colo, 1961](#); [Dresnay, 1963](#); [Termier, 1936](#)) is made up of two thick limestone bars (15 to 20 m) with shelf deposits very rich in neritic fauna including corals, lamellibranchs, gastropods and ammonites. The late Bajocian age attributed by [Termier \(1936\)](#) is confirmed by *Flabellothyris oranensis* associated with *Ermoceras* ([Choubert and Faure-Muret, 1967](#); [Rousselle, 1963, 1965](#)). This formation is therefore considered basal late Bajocian in age, Niortense Zone ([Alméras et al., 2007](#)).

Ich Timellaline/Bou Akrabene Formation ([Dresnay, 1963](#)) this formation mainly consists of oolitic and bioclastic limestones alternating with marly limestones and marls and ends with a sandstone bar “Aïn Brel Sandstones” denoting the end of the shelf carbonate deposits ([Fig. 2](#)). Thus far, the formation has yielded abundant and diverse marine fauna including small-branched corals, echinoids, bivalves and endemic brachiopods (Rhynchonellids, Terebratulides, Zeilleriids; see [Colo, 1961](#)). These strata are thought to have been deposited in an open relatively shallow marine environment. This formation is locally dated to the *Parkinsoni* Zone and has delivered brachiopods (*Burmirhynchia athiensis*) associated with ammonites (*Parkinsonia* sp., [Fig. 2, point 1](#)) indicating the late Bajocian–early Bathonian ([Alméras et al., 2007](#); [Rousselle, 1965](#)).

El Mers Group consists of three formations ([Charrière, 1989, 1990](#)): *i*) **El Mers 1 Fm.** is characterized by its reddish-purple marls indicating the first continental influences. In addition, it is renowned for its abundance of dinosaur remains collected in the nearby El Mers syncline ([Dresnay, 1963](#); [Lapparent, 1955](#)). In this same syncline, an intercalated marine level raises an endemic ammonite *Cadomites bremeri* ([Fig. 2, point 2](#)), indicating a middle Bathonian age ([Fedan, 1993](#)). Only the basal part of this formation is represented in the studied section. *ii*) **El Mers 2 Fm.** unconformably overlies the El Mers 1 fm. and displays internal bed strains reflecting synsedimentary basin deformations ([Dresnay, 1969](#); [Charrière, 1990](#); [Fedan, 1993](#)). The El Mers 2 fm. is made of decametric sequences with internal shelf marls alternating by intertidal sandstones. The sequence contains foraminifers, *Pseudocyathamina maynci* ([Fig. 2, point 3](#)), which is a middle Bathonian–Callovian index fossil ([Charrière, 1990](#)). *iii*) **El Mers 3 Fm.** consists of evaporitic facies representing the latest Jurassic deposits covered by the Early Cretaceous sedimentation.

3. Material and methods

The studied section is located in the southwestern block of the Taferdouste NW-SE dextral thrust, southeast of the mapped point 1635 (Jbel Brel) ([Figs. 1C and 3](#)). The FD section, about 390 m thick, is located along the main road between the Skoura and Boulemane cities.

A total of 117 rocks are sampled, one from the Recifa Formation (FD1), 107 mostly recovered from the marly, marly limestone and limestone beds of the Ich Timellaline/Bou Akrabene Formation (FD2-FD108) and nine samples from the overlying El Mers 1 Formation (FD109-FD117).

After washing and drying, the standard processing involved chemical treatment of 60 g of the sample with hydrochloric acid (HCl-37%) to eliminate carbonate fraction followed by hydrofluoric acid attack (HF-40%) to remove silicates. Residues were sieved using a 15 µm nylon mesh and the remaining material was centrifuged. The palynological slides containing the organic matter were mounted using glycerol gelatin. Two microscope slides were prepared for each sample for dinoflagellate cyst analysis. Whole slides of residues were investigated under a binocular transmitted light microscope (Leica optical

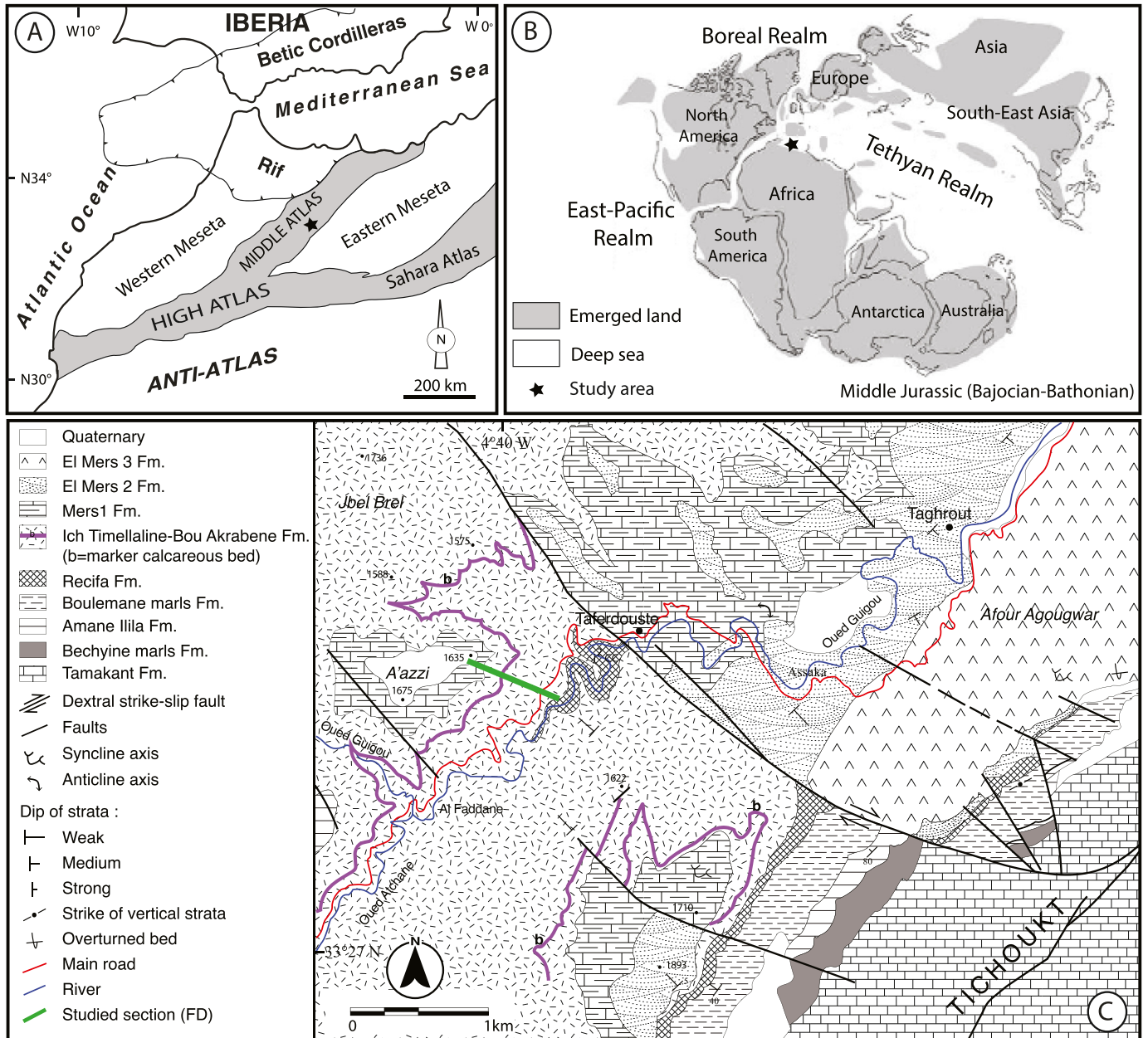


Fig. 1. A. Location of the Middle Atlas. B. Principal palaeogeographic units during Bajocian/Bathonian transition, with the location of the study area (modified from Moyne and Neige, 2007). C. Simplified geological map of the Skoura syncline (Middle Atlas, Morocco), with the location of the studied section (after Oukassou et al., 2016).

microscope equipped with a Leica DFC450C digital Camera) to identify and count palynomorphs and other organic matter components (amorphous organic matter, ligneous and carbonaceous phytoclasts...). The palynological slides are stored at the Department of Geology of the Faculty of Sciences Ben M'sick, Hassan II University of Casablanca, Morocco.

The qualitative and quantitative study included palynofacies analysis of organic matter (Table 1; Figs. 4, 6, 7 and 8). The relative percentage of these components is based on counting at least 300 particles per slide. The organic matter is grouped into: *i*) a continental fraction including phytoclasts (opaque and translucent), pollen grains and spores, *ii*) a marine fraction composed of organic-walled dinoflagellate cysts, foraminiferal linings and acritarchs, and *iii*) amorphous organic matter (AOM).

Two palynofacies parameters were derived from the data and used for interpretation: the AOM-Phytoclast-Palynomorph content plotted in a diagram (Figs. 6 and 8); and the (S/D) ratio representing the relative influences of sporomorphs (spores and pollen) over marine organic

material (dinoflagellate cysts, acritarchs), this ratio was calculated using the equation: $[S/D = nS / (nD + nS)]$ (Versteegh, 1994) (Fig. 7).

4. Results and discussion

4.1. Biostratigraphy

The palynological analysis of 109 samples collected in the FD section revealed the presence of well-preserved organic matter. Among them, fifty-eight contained rich and diverse palynomorph assemblages, dominated by spores and pollen grains (ranges between 15.9% and 84.6%, Fig. 7). They are represented essentially by inaperturate pollen grains, bissacates, smooth spores (*Cyathidites*, *Deltoisporites*), *Araucariacites*, *Callialasporites* (*C. dampieri*, *C. turbatus* and *C. segmentatus*) and *Classopollis*. Dinoflagellate cysts are few to common; they range between 9.34% and 26.81% of total palynomorphs, but can occasionally

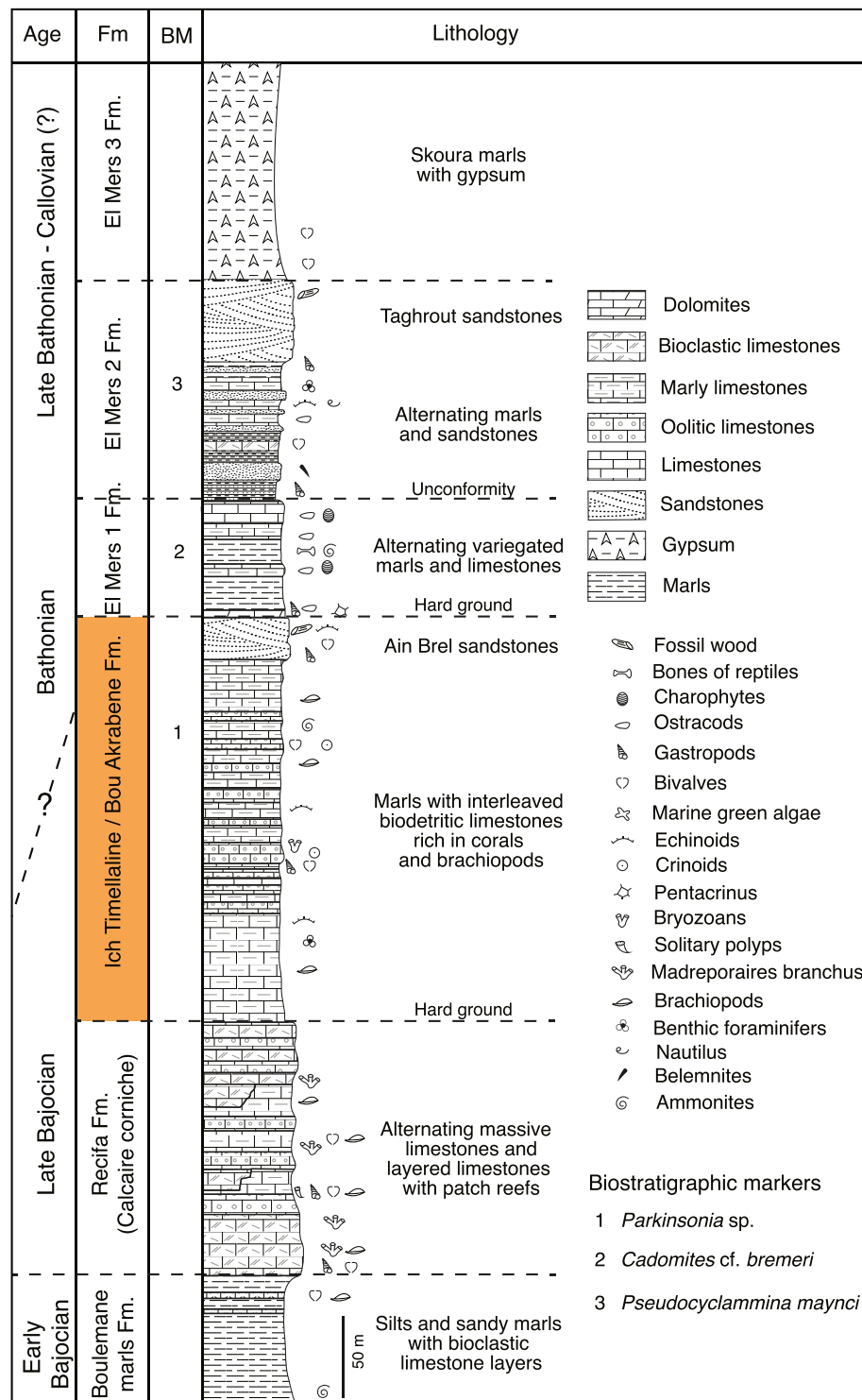


Fig. 2. Lithostratigraphic subdivision of the Middle Jurassic strata of the Skoura syncline (Middle Atlas, Morocco), with some biostratigraphic markers (Oukassou, 2018).

be abundant in the upper part of the section (between FD99 and FD107) where they can reach 66.93% of total palynomorphs. Foraminiferal wall linings are common between samples FD1 and FD88 reaching 32.5% in sample FD62. Their relative abundances decrease between samples FD88 and FD107 where they do not exceed 8.12%. Other marine palynomorphs, such as acritarchs (mainly *Micrhystridium* spp. genus and some specimens of *Veryhachium* spp. Fig. 7) are rare (3.14%).

Prasinophytes are represented essentially by Tasmanacea and they rarely attain 15% between samples FD1 and FD88 (Fig. 7). We recognized also a second type of palynofacies contained in forty-six samples collected in limestone beds. These samples are palynologically barren containing phytoclasts represented by structured opaque particles derived from oxidized black woody tissues (see paragraphs 4.2 and 4.4 for more detail).

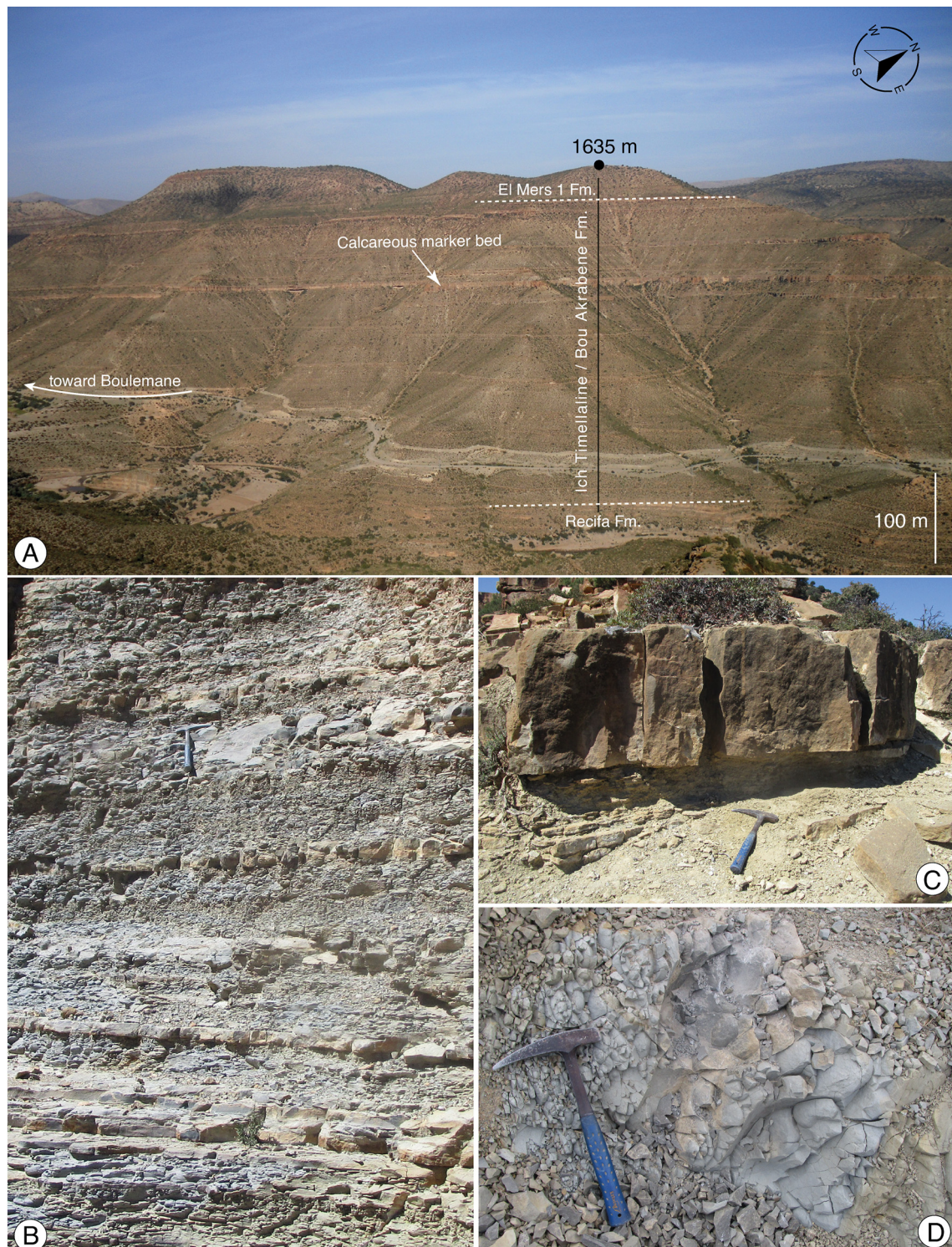


Fig. 3. FD section from Skoura syncline (Middle Atlas, Morocco): A. Panoramic view on the outcrop of the FD section (See Fig. 1C). B. General aspect of the marly-limestones of the median part of the FD section. C. Detail of oolitic limestone of the uppermost part of the Ich Timellaline/Bou Akrabene Fm. D. Note the grayish color of marls in the lower part of the Ich Timellaline/Bou Akrabene Fm.

In this work, age assessment is based primarily on ranges of dinoflagellate cysts. We recognized 68 dinoflagellate cyst species belonging to 36 genera, of which 8 are good late Bajocian–early Bathonian markers (Table 1). Our biostratigraphic subdivision is based on the well-known Bajocian and Bathonian First Occurrence (FO) and Last Occurrence (LO) datums of worldwide high-resolution biostratigraphic markers (Table 1 and Fig. 4). Comparisons with dinoflagellate cyst assemblages

in the Subboreal domain, particularly the northwest of Europe (Poulsen and Riding, 2003; Riding and Thomas, 1992; Woollam and Riding, 1983); in the Tethyan domain (Correia et al., 2018; Hssaïda et al., 2017; Ibrahim et al., 2001; Mafi et al., 2013) and in the Austral domain (Riding et al., 2010) (Fig. 5), have allowed the biostratigraphic and paleoenvironmental subdivision of the Bajocian and Bathonian deposits of the Skoura syncline. Two palynological biozones have been identified

Table 1

List and numerical distribution of the recorded dinoflagellate cysts on the FD section of the Skoura syncline (Middle Atlas, Morocco).

System		Epoch		Stage		Early Bathonian		Middle Jurassic		Late Bajocian		Ich Timmeline/Bau Akrabene			
Formations		Samples													
El Mers I	FD117	1. <i>Dinorites davisi</i>		2. <i>Costatohauerius</i> spp.		3. <i>Micarangoonyalas cf. weniai</i>		4. <i>Cibospiraeditum regnum</i>		5. <i>Dissiditidium</i> , sp?		6. <i>Korycetes</i> spp		7. <i>Dissiditidium minimum</i>	
	FD110	8. <i>Centiditidium</i> spp		9. <i>Dissiditidium</i> spp		10. <i>Elyptilites</i> <i>Vittensis</i> (<i>group</i>)		11. <i>Meiarangoonyalas</i> spp		12. <i>Dicroidia</i> <i>pyrularia</i> <i>sphenoidii</i>		13. <i>Edenites</i> <i>ovalum</i>		14. <i>Ceratoditidium cornigerum</i>	
	FD109	15. <i>Endosetium</i> spp		16. <i>Meiarangoonyalas weniai</i>		17. <i>Dissiditidium arenatum</i>		18. <i>Dissiditidium</i> sp?		19. <i>Paraceraspisites</i> <i>cerithophora</i>		20. <i>Reticulopora</i> spp		21. <i>Goniatites</i> <i>jurassica</i>	
	FD108	22. <i>Dissiditidium</i> <i>granatum</i>		23. <i>Lepiditidium</i> spp		24. <i>Kedipites</i> <i>segeta</i>		25. <i>Uvularia</i> <i>venula</i>		26. <i>Caryocyrtus</i> <i>gobii</i>		27. <i>Aldorphoridium</i> spp		28. <i>Polydorites</i> <i>regalis</i>	
	FD107	29. <i>Keypetes</i> sp?		30. <i>Ceropora</i> <i>cf. criciformis</i>		31. <i>Sensibilites</i> spp		32. <i>Cavatulites</i> <i>lentatum</i> sp?		33. <i>Meiarangoonyalas</i> spp		34. <i>Goniatites</i> <i>praelepis</i>		35. <i>Dissiditidium</i> <i>primum</i>	
	FD106	36. <i>Rhytidoditidium</i> spp		37. <i>Tanaria</i> <i>arcifera</i>		38. <i>Plagiotrigona</i> <i>stictum</i>		39. <i>Tabularicella</i> <i>dangerdii</i>		40. <i>Ceratoditidium</i> <i>orbiculatum</i>		41. <i>Teichoditidium</i> spp		42. <i>Meiarangoonyalas</i> sp?	
	FD105	43. <i>Epiphaphores</i> spp		44. <i>Tribolites</i> <i>scabellense</i>		45. <i>Versicolorites</i> <i>praelimma</i>		46. <i>Goniatites</i> <i>ebenaki</i>		47. <i>Ceropora</i> <i>venustum</i>		48. <i>Ceratoditidium</i> <i>conticum</i>		49. <i>Meiarangoonyalas</i> <i>caenorhinis</i>	
	FD104	50. <i>Elyptilites</i> <i>giganteus</i>		51. <i>Rhytidoditidium</i> <i>deplanata</i>		52. <i>Sensibilites</i> <i>rothi</i>		53. <i>Miliolidium</i> spp		54. <i>Goniatites</i> <i>jurassica</i> subsp. <i>ebenaki</i>		55. <i>Semibalanites</i> sp?		56. <i>Paraceraspisites</i> spp	
	FD103	57. <i>Bridgellites</i> <i>adella</i>		58. <i>Meiarangoonyalas</i> <i>relicta</i>		59. <i>Meiarangoonyalas</i> sp?		60. <i>Goniatites</i> <i>jurassica</i> subsp. <i>ebenaki</i>		61. <i>Ectenites</i> <i>ebenaki</i> sp?		62. <i>Meiarangoonyalas</i> <i>cf. effimerae</i>		63. <i>Ammonites</i> <i>symmetrum</i>	
	FD102	64. <i>Spiriferites</i> <i>orbicularis</i>		65. <i>Indosetium</i> <i>omatum</i>		66. <i>Goniatites</i> <i>jurassica</i> subsp. <i>longicornis</i>		67. <i>Ceratoditidium</i> <i>omatum</i>		68. <i>Meiarangoonyalas</i> <i>cf. exponens</i>		69. <i>Meiarangoonyalas</i> <i>cf. valenciennesi</i>		70. <i>Goniatites</i> <i>jurassica</i> subsp. <i>ebenaki</i>	
Ich Timmeline	FD78	1. 2. 1. 2. 2. 2. 2. 1.		3. 1. 1. 1.		4. 1. 2. 1. 1. 1.		5. 1. 2. 2. 1. 1.		6. 1. 2. 2. 1. 1.		7. 1. 2. 2. 1. 1.		8. 1. 2. 2. 1. 1.	
	FD77	9. 1. 1. 1. 1. 1. 1. 1.		10. 1. 1. 1. 1. 1. 1. 1.		11. 1. 1. 1. 1. 1. 1. 1.		12. 1. 1. 1. 1. 1. 1. 1.		13. 1. 1. 1. 1. 1. 1. 1.		14. 1. 1. 1. 1. 1. 1. 1.		15. 1. 1. 1. 1. 1. 1. 1.	
	FD76	16. 1. 1. 1. 1. 1. 1. 1.		17. 1. 1. 1. 1. 1. 1. 1.		18. 1. 1. 1. 1. 1. 1. 1.		19. 1. 1. 1. 1. 1. 1. 1.		20. 1. 1. 1. 1. 1. 1. 1.		21. 1. 1. 1. 1. 1. 1. 1.		22. 1. 1. 1. 1. 1. 1. 1.	
	FD67	23. 1. 1. 1. 1. 1. 1. 1.		24. 1. 1. 1. 1. 1. 1. 1.		25. 1. 1. 1. 1. 1. 1. 1.		26. 1. 1. 1. 1. 1. 1. 1.		27. 1. 1. 1. 1. 1. 1. 1.		28. 1. 1. 1. 1. 1. 1. 1.		29. 1. 1. 1. 1. 1. 1. 1.	
	FD66	30. 1. 1. 1. 1. 1. 1. 1.		31. 1. 1. 1. 1. 1. 1. 1.		32. 1. 1. 1. 1. 1. 1. 1.		33. 1. 1. 1. 1. 1. 1. 1.		34. 1. 1. 1. 1. 1. 1. 1.		35. 1. 1. 1. 1. 1. 1. 1.		36. 1. 1. 1. 1. 1. 1. 1.	
	FD65	37. 1. 1. 1. 1. 1. 1. 1.		38. 1. 1. 1. 1. 1. 1. 1.		39. 1. 1. 1. 1. 1. 1. 1.		40. 1. 1. 1. 1. 1. 1. 1.		41. 1. 1. 1. 1. 1. 1. 1.		42. 1. 1. 1. 1. 1. 1. 1.		43. 1. 1. 1. 1. 1. 1. 1.	
	FD64	44. 1. 1. 1. 1. 1. 1. 1.		45. 1. 1. 1. 1. 1. 1. 1.		46. 1. 1. 1. 1. 1. 1. 1.		47. 1. 1. 1. 1. 1. 1. 1.		48. 1. 1. 1. 1. 1. 1. 1.		49. 1. 1. 1. 1. 1. 1. 1.		50. 1. 1. 1. 1. 1. 1. 1.	
	FD63	51. 1. 1. 1. 1. 1. 1. 1.		52. 1. 1. 1. 1. 1. 1. 1.		53. 1. 1. 1. 1. 1. 1. 1.		54. 1. 1. 1. 1. 1. 1. 1.		55. 1. 1. 1. 1. 1. 1. 1.		56. 1. 1. 1. 1. 1. 1. 1.		57. 1. 1. 1. 1. 1. 1. 1.	
	FD62	58. 1. 1. 1. 1. 1. 1. 1.		59. 1. 1. 1. 1. 1. 1. 1.		60. 1. 1. 1. 1. 1. 1. 1.		61. 1. 1. 1. 1. 1. 1. 1.		62. 1. 1. 1. 1. 1. 1. 1.		63. 1. 1. 1. 1. 1. 1. 1.		64. 1. 1. 1. 1. 1. 1. 1.	
Ich Timmeline	FD61	65. 1. 1. 1. 1. 1. 1. 1.		66. 1. 1. 1. 1. 1. 1. 1.		67. 1. 1. 1. 1. 1. 1. 1.		68. 1. 1. 1. 1. 1. 1. 1.		69. 1. 1. 1. 1. 1. 1. 1.		70. 1. 1. 1. 1. 1. 1. 1.		71. 1. 1. 1. 1. 1. 1. 1.	
	FD60	72. 1. 1. 1. 1. 1. 1. 1.		73. 1. 1. 1. 1. 1. 1. 1.		74. 1. 1. 1. 1. 1. 1. 1.		75. 1. 1. 1. 1. 1. 1. 1.		76. 1. 1. 1. 1. 1. 1. 1.		77. 1. 1. 1. 1. 1. 1. 1.		78. 1. 1. 1. 1. 1. 1. 1.	
	FD59	79. 1. 1. 1. 1. 1. 1. 1.		80. 1. 1. 1. 1. 1. 1. 1.		81. 1. 1. 1. 1. 1. 1. 1.		82. 1. 1. 1. 1. 1. 1. 1.		83. 1. 1. 1. 1. 1. 1. 1.		84. 1. 1. 1. 1. 1. 1. 1.		85. 1. 1. 1. 1. 1. 1. 1.	
	FD58	86. 1. 1. 1. 1. 1. 1. 1.		87. 1. 1. 1. 1. 1. 1. 1.		88. 1. 1. 1. 1. 1. 1. 1.		89. 1. 1. 1. 1. 1. 1. 1.		90. 1. 1. 1. 1. 1. 1. 1.		91. 1. 1. 1. 1. 1. 1. 1.		92. 1. 1. 1. 1. 1. 1. 1.	
	FD57	93. 1. 1. 1. 1. 1. 1. 1.		94. 1. 1. 1. 1. 1. 1. 1.		95. 1. 1. 1. 1. 1. 1. 1.		96. 1. 1. 1. 1. 1. 1. 1.		97. 1. 1. 1. 1. 1. 1. 1.		98. 1. 1. 1. 1. 1. 1. 1.		99. 1. 1. 1. 1. 1. 1. 1.	
	FD56	100. 1. 1. 1. 1. 1. 1. 1.		101. 1. 1. 1. 1. 1. 1. 1.		102. 1. 1. 1. 1. 1. 1. 1.		103. 1. 1. 1. 1. 1. 1. 1.		104. 1. 1. 1. 1. 1. 1. 1.		105. 1. 1. 1. 1. 1. 1. 1.		106. 1. 1. 1. 1. 1. 1. 1.	
	FD55	107. 1. 1. 1. 1. 1. 1. 1.		108. 1. 1. 1. 1. 1. 1. 1.		109. 1. 1. 1. 1. 1. 1. 1.		110. 1. 1. 1. 1. 1. 1. 1.		111. 1. 1. 1. 1. 1. 1. 1.		112. 1. 1. 1. 1. 1. 1. 1.		113. 1. 1. 1. 1. 1. 1. 1.	
	FD54	114. 1. 1. 1. 1. 1. 1. 1.		115. 1. 1. 1. 1. 1. 1. 1.		116. 1. 1. 1. 1. 1. 1. 1.		117. 1. 1. 1. 1. 1. 1. 1.		118. 1. 1. 1. 1. 1. 1. 1.		119. 1. 1. 1. 1. 1. 1. 1.		120. 1. 1. 1. 1. 1. 1. 1.	
	FD53	121. 1. 1. 1. 1. 1. 1. 1.		122. 1. 1. 1. 1. 1. 1. 1.		123. 1. 1. 1. 1. 1. 1. 1.		124. 1. 1. 1. 1. 1. 1. 1.		125. 1. 1. 1. 1. 1. 1. 1.		126. 1. 1. 1. 1. 1. 1. 1.		127. 1. 1. 1. 1. 1. 1. 1.	
	FD52	128. 1. 1. 1. 1. 1. 1. 1.		129. 1. 1. 1. 1. 1. 1. 1.		130. 1. 1. 1. 1. 1. 1. 1.		131. 1. 1. 1. 1. 1. 1. 1.		132. 1. 1. 1. 1. 1. 1. 1.		133. 1. 1. 1. 1. 1. 1. 1.		134. 1. 1. 1. 1. 1. 1. 1.	
Recife	FD1	135. 1. 1. 1. 1. 1. 1. 1.		136. 1. 1. 1. 1. 1. 1. 1.		137. 1. 1. 1. 1. 1. 1. 1.		138. 1. 1. 1. 1. 1. 1. 1.		139. 1. 1. 1. 1. 1. 1. 1.		140. 1. 1. 1. 1. 1. 1. 1.		141. 1. 1. 1. 1. 1. 1. 1.	

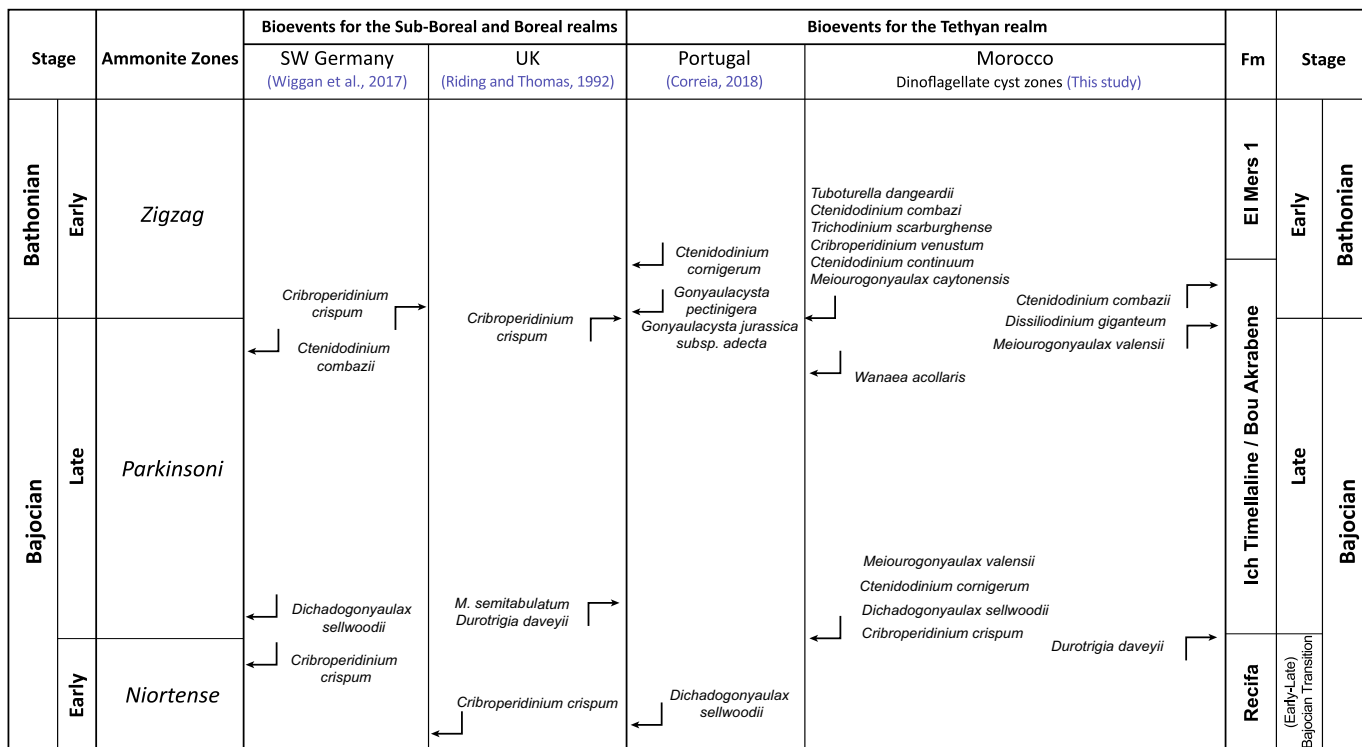


Fig. 4. Stratigraphical distribution of late Bajocian-early Bathonian dinoflagellate cyst events in Sub-boreal, Boreal and Tethyan realms against ammonite zones. Arrows mark first appearances and last appearances of species.

in the studied interval based on the stratigraphic ranges of dinoflagellate cysts. Each zone is named after marker species having ranges that are entirely within the zones.

4.1.1. Assemblage biozone *Ctenidodinium cornigerum* and *Cribroperidinium crispum* (CC/CC)

This biozone encompasses samples FD1-FD100 (340 m) between the base of Recifa Formation (early Bajocian-late Bajocian transition) and the Ich Timellaline/Bou Akrabene Formation (late Bajocian-early Bathonian). The base of this biozone is defined by the first occurrences of *Cribroperidinium crispum* and *Ctenidodinium cornigerum*, the last occurrences of *Durotrigia daveyii*. Its top is defined by the last occurrences of *Cribroperidinium crispum* and *Meiourogonyaulax valensi*, the first occurrences of *Ctenidodinium combazi* and *Cribroperidinium venustum* (Table 1 and Fig. 4).

4.1.1.1. Early Bajocian–late Bajocian transition (base of the assemblage biozone CC/CC). Sample FD1 is assigned to the early Bajocian–late Bajocian transition, based on the relevant dinoflagellate cyst events: the FOs of *Ctenidodinium cornigerum*, *Cribroperidinium crispum* and the LO of *Durotrigia daveyii*. The assemblage of relatively low diversity encompassing *Dissiliodinium* spp., *Sentusidinium*/*Ellepsoidictyum* group, *Meiourogonyaulax* spp., *Ctenidodinium* spp., *Cribroperidinium* spp., *Ctenidodinium cornigerum*, *Dichadogonyaulax sellwoodii*, *Valensiella ovulum*, *Cassiculosphaeridium* and *Durotrigia daveyii* (Table 1). *Durotrigia daveyii* has never exceeded the late Bajocian in several localities (Bailey, 1987; Feist-Burkhardt, 1990; Feist-Burkhardt and Monteil, 1997; Fensome et al., 1993; Riding and Thomas, 1992; Riding et al., 1991; Wiggan et al., 2017). The cosmopolitan species *Dichadogonyaulax sellwoodii* was recorded within the late Bajocian (Fig. 4) (Herngreen and De Boer, 1984; Riding et al., 1991; Feist-Burkhardt and Wille, 1992; Riding and Thomas, 1992; Fenton et al., 1994, 1995; Fensome et al., 1996; Feist-Burkhardt and Monteil, 1997). It has been recorded in the early-late Bajocian transition at the top of *S. humphriesianum* Ammonite Zone in the southwest of Germany (Wiggan et al., 2017). This is

supported by the presence of two late Bajocian marker taxa *Ctenidodinium cornigerum* and *Cribroperidinium crispum* (Fenton, 1981; Woollam and Riding, 1983; Feist-Burkhardt and Monteil, 1997). *Durotrigia daveyii* has never exceeded the late Bajocian in several localities (Bailey, 1987; Feist-Burkhardt, 1990; Feist-Burkhardt and Monteil, 1997; Fensome et al., 1993; Riding et al., 1991; Riding and Thomas, 1992; Wiggan et al., 2017). Therefore, the Lower–Upper Bajocian boundary lies at the base of the section in sample FD1 (Recifa Fm.).

Our assemblage shares similarities with those described by Feist-Burkhardt (1990), Riding and Thomas (1992), Fensome et al. (1993), Wiggan et al. (2017) from the early-late Bajocian of Subboreal realm, providing a correlation between the base of CC/CC Zone recognized in the Recifa Fm in Morocco and the DSJ13/DSJ14 of northwest Europe previously recorded by Poulsen and Riding (2003) (Fig. 5). The main difference being the absence of *Nannoceratopsis* genus from the FD section. Despite the presence of characteristic endemic dinoflagellate cyst assemblages in the Austral realm, the base of CC/CC Zone in the FD section coincides with the *Nannoceratopsis deflandrei* Zone documented by Riding et al. (2010) in northwest Australia. Correlation of the studied section with its contemporaneous deposits in the Austral realm revealed a similarity in the biostratigraphic range of some dinoflagellate cyst taxa during the early-late Bajocian transition, including *Cribroperidinium cf. crispum*, *Ctenidodinium* spp. and *Dissiliodinium* spp.

4.1.1.2. Late Bajocian (assemblage biozone *Ctenidodinium cornigerum* and *Cribroperidinium crispum* CC/CC). Late Bajocian, from sample FD2 to sample FD100, extends on 335 m (Table 1). This interval is part of the Ich Timellaline/Bou Akrabene Fm. The recognition of the age is based on several global dinoflagellate cyst events: simultaneous and progressive appearances of taxa, plus their acmes. This zone is marked by the first appearances of *Meiourogonyaulax valensi*, *Korystocysta gochtii*, *Dichadogonyaulax sellwoodii*, *Dissiliodinium* spp., *Cribroperidinium* spp., *Gonyaulacysta pectinigera* and *Ctenidodinium cornigerum* (Table 1; Fig. 4). The last two taxa are considered as excellent marker taxa of the late Bajocian (Feist-Burkhardt and Monteil, 1997; Fenton, 1981;

Stage		Ammonite Zones	Australian realm	Sub-Boreal and Boreal realms			Tethyan realm			
				Australia (Riding et al., 2010)	Denmark and UK (Poulsen and Riding, 2003)	UK (Riding and Thomas, 1992)	Iran (Mafi, 2013)	Egypt (Ibrahim, 2001)	Morocco (Hssaida, 2017)	Morocco (This study)
Bajocian	Bathonian	Zigzag	<i>Wanaea indotata</i>	<i>Dichadogonyaulax sellwoodii</i>	DS15	<i>Dichadogonyaulax sellwoodii</i>	a	<i>Dichadogonyaulax sellwoodii</i>	<i>Dichadogonyaulax sellwoodii</i>	The assemblage zone <i>Ctenidodinium combazii</i> <i>Dichadogonyaulax sellwoodii</i>
	Early									The assemblage zone <i>Ctenidodinium combazii</i> <i>Dichadogonyaulax sellwoodii</i>
	Late		<i>Wanaea verrucosa</i>	<i>Cribroperidinium crispum</i>	DS14	<i>Cribroperidinium crispum</i>	b	<i>Cribroperidinium crispum</i>	<i>Pareodinia ceratophora</i>	The assemblage zone <i>Ctenidodinium cornigerum</i> <i>Cribroperidinium crispum</i>
Early	Niortense	<i>Parkinsonia</i>	<i>Nannoceratopsis deflandrei</i>		DS13		a			

Fig. 5. Stratigraphic distribution of Bajocian–Bathonian dinoflagellate cyst biozones in Tethyan, Sub-boreal, Boreal and Australian realms against ammonite biozones.

Poulsen, 1998; Riding and Thomas, 1992; Wiggan et al., 2017; Woollam and Riding, 1983). *Ctenidodinium cornigerum* shows two successive highest relative abundances in samples FD28 and FD38, reaching 60% and 54.83% respectively. This is followed by the acme of *Dissiliodinium* genus in sample FD64 (64.07%) and the acme of *Meiourgonyaulax valensii* in sample FD96 (69.60%). The FO of the latter species is considered as a marker event of the late Bajocian in the Northern Hemisphere (Williams and Bujak, 1985). The presence of *Dichadogonyaulax sellwoodii* and the successive FOs of *Korystocysta gochtii* and *Gonyaulacysta pectinigera* indicate also late Bajocian age to this sample interval since their FOs are considered as biostratigraphic marker events of the late Bajocian (Fenton, 1981; Woollam and Riding, 1983). Other taxa also occur in this interval and show stratigraphic interest including *Endoscrinium* spp., *Wanaea acollaris*, *Leptodinium* spp. and *Aldorfia aldorfensis*. Despite their low occurrences in this interval (1 to 3 specimens), these species are known to characterize the late Bajocian. They were recognized in the late Bajocian of northwest Europe, such as in France, Germany and England (Fauconnier, 1995; Feist-Burkhardt and Wille, 1992; Poulsen, 1998; Riding and Thomas, 1992; Williams et al., 1993). This interval contains few long-ranging species, such as *Pareodinia ceratophora*, *Gonyaulacysta jurassica*, *Meiourgonyaulax* spp., *Ctenidodinium* spp. and *Valensiella/Ellipsoidictium* group. The CC/CC dinoflagellate cyst biozone could be correlated with the *Cribroperidinium crispum* Zone of Riding and Thomas (1992) (Fig. 5) and the DS14 Zone defined in northwest Europe (Subboreal domain) by Poulsen and Riding (2003). *Cribroperidinium crispum* Zone has been recorded in the Tethyan domain, particularly in Iran (Mafi et al., 2013) (Fig. 5); this zone is synchronous to *Pareodinia ceratophora* Zone recorded in Egypt (El Beialy and Ibrahim, 1997) and to *Dichadogonyaulax sellwoodii* Zone identified in Israel (Conway, 1990). The species composition of these biozones recovered in the Subboreal and Tethyan domains shows a close resemblance. These species are *Dissiliodinium* spp., *D. sellwoodii*, *C. cornigerum*, *Valensiella ovulum*, *G. jurassica*, *C. crispum*, *M. valensii*, *P. ceratophora*, *Kallosphaeridium* spp. and *Batiacasphaera* spp. Despite this similarity, some significant compositional differences are found. Cosmopolitan species of *Nannoceratopsis* such as *Nannoceratopsis gracilis* appear to be common during the late Bajocian in both Tethyan and Subboreal realms (Ghasemi-Nejad et al., 2012; Riding,

1984; Riding and Thomas, 1992). However, the genus *Nannoceratopsis* has not been recorded in Moroccan sediments. Other taxa, encountered in the Bajocian in the Tethyan realm such as in Northwest Europe (Feist-Burkhardt, 1990; Wiggan et al., 2017) and in the late Bajocian–early Bathonian in Middle Atlas of Morocco (present study), are apparently absent from Bajocian deposits of Portugal (Correia et al., 2018) (Fig. 5).

The Tethyan index species, *Ctenidodinium cornigerum*, is considered to be of biostratigraphic importance. It has a Bajocian–Bathonian transition range (Jan de Chene et al., 1985; Feist-Burkhardt and Monteil, 1997; Wiggan et al., 2017). In the Middle Atlas, this species is consistently present throughout the FD section (Table 1). In this section, the CC/CC biozone is equivalent to the *Wanaea verrucosa* Zone of Riding et al. (2010) spanning the late Bajocian–early Bathonian in the Austral realm (Fig. 5). It is characterized by the presence of endemic association, including *Endoscrinium kempiae*, *Nannoceratopsis* spp., *Pareodinia ceratophora*, *Pareodinia halosa*, *Phallocysta granosa*, *T. balmei*, *Valvaeodinium spinosum*, *Wanaea enoda*, *Wanaea lacuna* and *W. verrucosa*, as well as *Pareodinia ceratophora* which occurs also in the CC/CC Zone.

4.1.2. Bajocian–Bathonian transition (Assemblage zone *Ctenidodinium combazii* and *Dichadogonyaulax sellwoodii* CC/DS)

The Bajocian–Bathonian transition has been recognized from sample FD100 to sample FD109. It extends on 22 m from the top of Ich-Timella line/Bou Akrabene to the base of the El Mers 1 Formation (Table 1). The base of the CC/DS Zone is defined by the last occurrences of *Cribroperidinium crispum*, *Meiourgonyaulax valensii*, and the first occurrences of *Ctenidodinium combazii*, *Meiourgonyaulax caytonensis*, *Cribroperidinium venustum*, *Trichodinium scarburghense*, *Korystocysta pachyderma*, *Ctenidodinium continuum*, *Rhynchodiniopsis cladophora* and *Cribroperidinium venustum*, followed by the FOs of *Willeidinium* spp., *Aldorfia aldorfensis* in sample FD 101 and *Meiourgonaulax reticulata* in sample FD 102 (Figs. 4 and 5). Other associated species appear in this interval such as *Tubotuberella dangeardii*, which characterizes the Bajocian age (Poulsen, 1998; Riding, 1983; Wiggan et al., 2017). In the FD section, species whose LO was recorded in the late Bajocian such as *Cribroperidinium crispum* is associated with early Bathonian marker taxa, such as *Cribroperidinium venustum*,

Trichodinium scarburghense, *Korystocysta pachyderma*, *Ctenidodinium continuum*, *Rhynchodiniopsis cladophora*, *Aldorfia aldorfensis* and *Meiourogonaulax reticulata* (Table 1). Therefore, the Bajocian–Bathonian boundary likely lies in this interval.

The palynological assemblage is dominated by species of *Ctenidodinium* (*Ctenidodinium sellwoodii*, *Ctenidodinium combazii* and *Ctenidodinium continuum*), *Dichadogonyaulax sellwoodii*, *Korystocysta gochtii*, *Korystocysta pochyderma* and *Wanaea acollaris*. Furthermore, this interval recorded a significant dominance of proximate cysts such as *Sentusidinium rioultii*, *Ellipsoidictyum cinctum* and *Endoscrinium gochtii* (Table 1). The abundance of the family Ctenidodinaceae and proximate cysts are characteristic of Early Bathonian in both the Subboreal realm (Poulsen and Riding, 2003; Riding, 1984; Smelror, 1993; Wiggan et al., 2017) and the Tethyan realm (Correia et al., 2018; Ghasemi-Nejad et al., 2012; Hssaida et al., 2017). The CC/DS Zone of Woollam and Riding (1983), marked by the presence of *Ctenidodinium combazii* in association with *Dichadogonyaulax sellwoodii*, is equivalent to CC/DS Zone encountered in the FD section. It characterizes the Bathonian age (Woollam and Riding, 1983; Riding and Thomas, 1992). *Dichadogonyaulax sellwoodii* is an excellent marker of the Bathonian, its acme characterizes the base of the Bathonian in both Subboreal and Tethyan realms. This acme was reported in the southwest of Germany (Wiggan et al., 2017); in England (Riding and Thomas, 1992), in Morocco (Hssaida, 1990; Hssaida et al., 2017), in the stratotype of Normandy (Hssaida, 1995) and in the present study (Fig. 5).

The CC/DS Zone, characterizing the early Bathonian, correlates with the assemblage zone defined by Hssaida et al. (2017) in the Guercif basin (northeast Morocco) (Fig. 5). Dinoflagellate cyst associations are similar in terms of occurrence and abundance of taxa. Principal differences include the presence of chorotrichous cysts such as *Adnatosphaeridium caulleryii* in the Guercif basin, it occurred also in the early Bathonian of the northwest Europe (Feist-Burkhardt and Wille, 1992; Riding et al., 1985). This species does not occur in Lower Bathonian sediments of the Middle Atlas (Morocco). The CC/DS zone correlates also with the *Dichadogonyaulax sellwoodii* defined by Mafi et al. (2013) in Iran and by El Beialy and Ibrahim (1997) in Egypt, characterizing the Bathonian age. However, Conway (1990) defined the *Wanaea acollaris* Zone for the Bathonian of Israel, which is equivalent to the *Dichadogonyaulax sellwoodii* Zone of Riding and Thomas (1992) and the *Ctenidodinium sellwoodii* of Poulsen and Riding (2003) defined for the northwest Europe.

4.2. Paleoenvironment

In this section, we discuss the palynofacies and the paleoenvironment through the vertical variation of organic matter components contained in the studied samples. Palynofacies is a term defined by Combaz (1964) to describe the total organic constituents obtained after processing using acids. The palynofacies analysis provides precious information on the sedimentary depositional environment and eustatic level changes controlling the sedimentation process.

For each sample, we counted 250 particles of marine and continental palynomorphs, phytoclasts and amorphous organic matter. The obtained results were plotted as relative frequency curves of the different organic components (Figs. 6 and 7) and reported on the ternary diagram of Tyson (1993, 1995) (Fig. 8).

The quantitative study of 109 samples from the FD section (Skoura Syncline, Middle Atlas of Morocco) allowed us to differentiate two categories of samples:

- The first category includes 51 samples (Figs. 6 and 8), in which the organic residue is exclusively composed of opaque, dark colored and structured fragments of phytoclasts without any internal structure that may represent highly oxidized and degraded coals called

inertinite (MOx) (Tyson, 1995). They refer to all oxidized or carbonized particles (Plate XII: 1). The 51 samples rich in phytoclasts are barren.

- The second category includes 58 samples (Fig. 7) containing amorphous organic matter (AOM), palynomorphs and phytoclasts. The latter, are yellow to brown, translucent and assigned to herbaceous material. These phytoclasts (Mob) are composed of translucent woody tissues and vegetal cells (cutinite) and lignin-rich tissues (vitrinite).

They are referred to all structured plant particles (Tyson, 1995; Batten and Koppelman, 1996; Carvalho, 2016). The Mob is abundant in all the 58 samples of this category (ranging between 11% and 86.66%), except at the top of the section in samples FD100, FD101 and FD102, where palynomorphs become dominant (15% and 17.7%). Amorphous organic matter (AOM) does not exceed 17.33% in these samples, it consists of non-structured, granular-textured and brown particles (Plate XII: 2). Palynomorphs (Fig. 7) are composed of spores and pollen grains with relative abundance ranging from 15.9% to 84.6%. Acratarchs are rare, they do not exceed 3.7%, in particular *Micrhystidium* spp. genus and some specimens of *Veryhachium* spp. Chitinous foraminiferal test linings show moderate relative abundances varying between 3.7% and 32.5%. Prasinophytes, Dasycladaceae and Leiosphaeridae algae (Tasmanites) appear also in these samples reaching up to 15.15%; finally, dinoflagellate cysts are rather more abundant ranging between 1.6% and 75.06%.

All the FD samples are plotted in palynofacies fields I, III and V from the ternary diagram of Tyson (1993, 1995) (Fig. 8). According to this author, field I corresponds to a proximal continental shelf; field III, points to an oxic-heterolithic continental shelf, with abundance of phytoclasts related to a proximate fluvio-deltaic sediment source; and field V refers to a distal continental shelf, in which palynomorphs are abundant and the amorphous organic matter proportions (usually degraded) are low to moderate.

The paleoenvironmental interpretation is based on the integration of all palynofacies parameters (the Ternary diagram of Tyson and the relative abundance changes of organic matter components, Figs. 6, 7 and 8). This data integration allows us to subdivide the FD section into 3 intervals:

- **Interval A:** defined between samples FD1 and FD38.

In this 170 m thick interval, 20 samples, containing only phytoclasts (MOx), are plotted in field I. Their high percentages are related to the proximity to terrestrial sources, they dominate areas close to the parent flora (Carvalho et al., 2016). The presence of these samples in field I indicates a proximal depositional environment, probably a marginal zone with low energy and anoxic conditions (Tyson, 1995). Other samples (18 samples) from this interval are distributed among fields III and V. The proportions of different palynofacies constituents (AOM, palynomorphs and phytoclasts) are shown in Fig. 6.

Phytoclasts (Mob), ranging between 37.66% and 82.28% in this interval, are mainly made up of wooden tracheid (Plate XII: 2). Their abundance is indicative of a significant continental flow associated with a proximal (coastal) environment (Carvalho et al., 2016; Pocklington and Leonard, 1979).

This is supported by the high abundance of sporomorphs oscillating from 31.81% to 79.66% (Fig. 7). They are dominated by non-saccate sporomorphs *Classopollis* (*Corollina* spp.), *Callialasporites* spp., *Araucariacites*, *Densosporites* spp., *Lycopodiumsporites* spp. and smooth-walled spores such as *Cyathidites* spp.). Saccates sporomorphs are extremely rare in these samples. According to Whitaker et al. (1992), thin-walled sporomorphs may be concentrated in the distal sediments. In contrast, non-saccate sporomorphs are relatively large, thick-walled, less buoyant and behave like sedimentary particles (sand

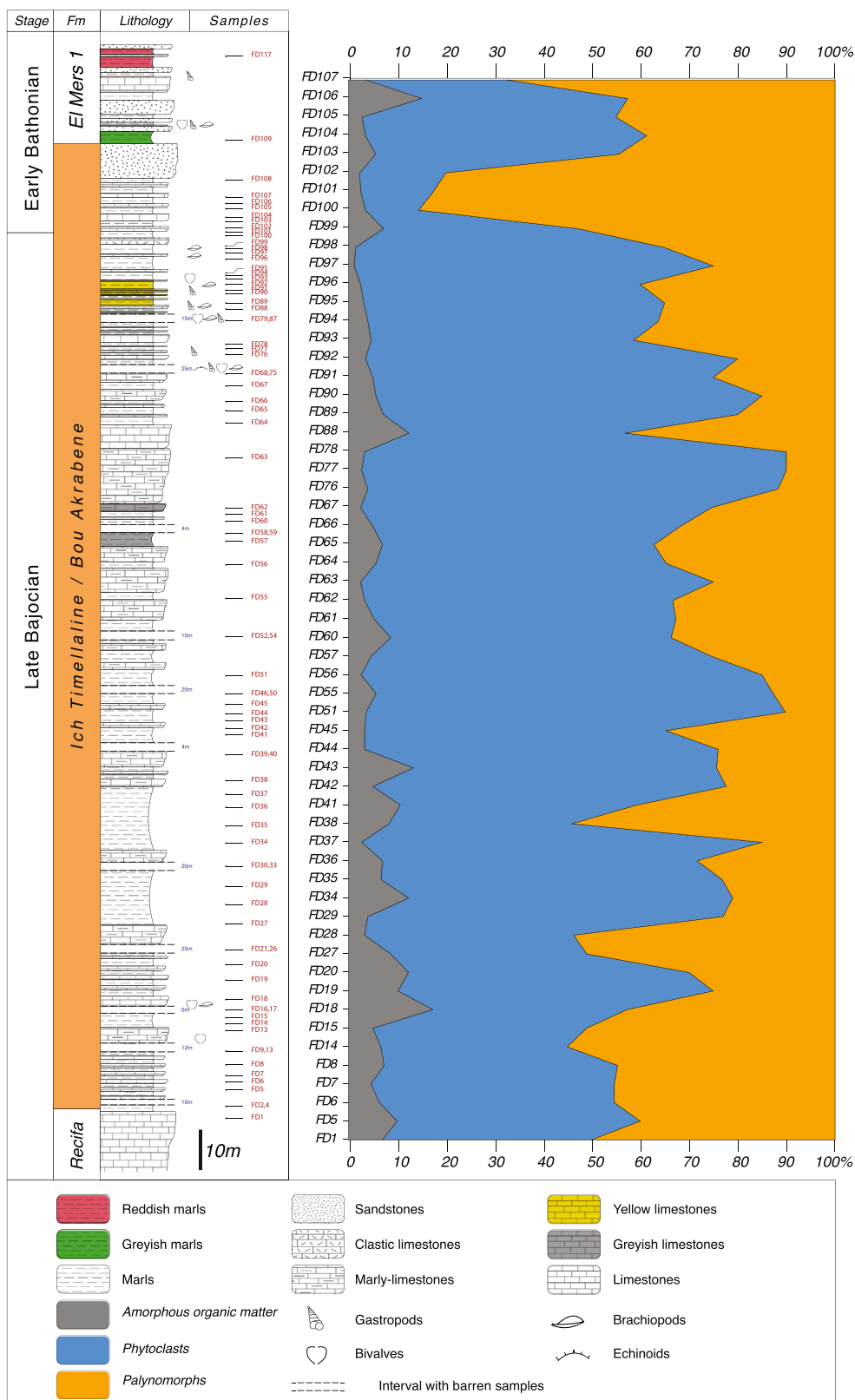


Fig. 6. Lithostratigraphic section (FD): lithology, sampled horizons and palynofacies data across the Upper Bajocian–Lower Bathonian formations of the Skoura syncline (Middle Atlas, Morocco).

or silt). They are more frequent near their source and constitute local marsh vegetation associated with coastal marine 'lagoon' environments. This supports the proximity to a continental source.

The dominance of non-saccate sporomorphs is coupled with the omnipresence of chitinous foraminiferal test linings (10% to 28%, Fig. 7). Their presence in association with prasinophytes, supports a shallow

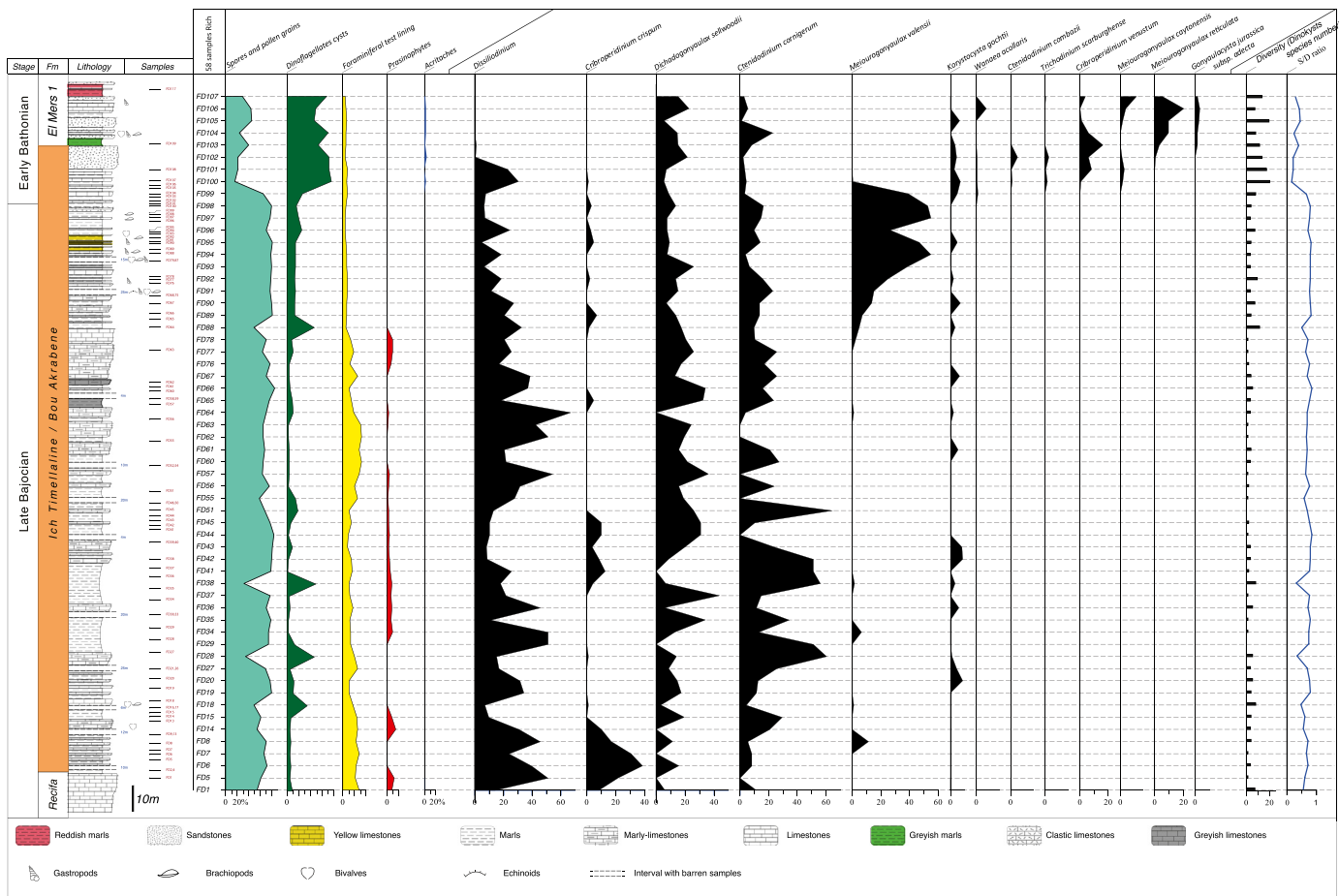


Fig. 7. Lithostratigraphic section (FD) and relative abundances, expressed as percentages, of the six main palynomorph groups across the Upper Bajocian- Lower Bathonian formations of the Skoura syncline (Middle Atlas, Morocco).

depositional environment (Batten and Dutta, 1997; Batten and Lister, 1988; Leckie and Singh, 1991).

The littoral/proximal character of samples belonging to interval A is further supported by a low relative abundance of dinoflagellate cysts not exceeding 12.22% (samples of field III). This is correlated with a low specific richness (not exceeding 19 species). The S/D ratio is between 0.31 and 0.79 (Fig. 7).

In this interval, dinoflagellate cysts show three successive peaks (Fig. 7): 34.44% (11 species) in sample FD18, 45.9% (9 species) in sample FD28 and 48.76% (12 species) in the FD38 sample. Three samples (FD8, FD28 and FD38) belong to field V in Tyson's (1993, 1995) diagram in association with samples (FD1, FD14 and FD27), indicating a distal continental shelf (Fig. 8). According to Tyson (1993, 1995), this may be related to marine incursions in the depositional environment. The increasing trend of dinoflagellate cysts has been already highlighted in Davey (1970) work on Cretaceous sequences from England, northern France and northern America. He demonstrates that the slight increase in dinoflagellate cyst abundance accompanied by an overall decrease in terrestrial organic matter concentration suggest a relative rise in sea level (Batten, 1999; Tyson, 1993, 1995).

In conclusion, interval A exhibits an oxic proximal/coastal paleoenvironment with significant terrigenous influx. It is marked by fluctuating marginal low-energy, stagnant, temporarily isolated environments from normal marine conditions (field I samples) and high-energy proximal-coastal environments (field III samples). Temporary marine incursions are highlighted by increasing marine fraction and dinoflagellate cyst abundance.

• Interval B: defined between samples FD39 and FD87.

This 190 m thick interval is represented by 49 samples dispersed among fields I and III (Fig. 8). The 29 samples within field I (Fig. 8) are mainly composed of MOx (Plate XII: 1), reflecting also a marginal proximal depositional environment as for the interval A. In contrast, field III includes 20 samples whose organic residues are dominated by phytoclasts (Mob) (between 48.67% and 87.3%) and sporomorphs (between 57.6% and 84.6%) (Figs. 6 and 7). The S/D ratio ranges between 0.49 and 0.84 (Fig. 7).

Sporomorphs are dominated mainly by *Classopollis* (*Corollina* spp.), *Callialasporites* spp. (including *Callialasporites dampieri*, *Callialasporites segmentatus* and *Callialasporites turbatus*), in association with *Araucariacites*, *Lycopodiumsporites* spp. and *Cyathidites* spp. These sporomorphs are more common close to their source and they are associated with coastal marine environments (Whitaker et al., 1992).

The presence of chitinous foraminifera (between 8.2% and 32.5%) and algae (prasinophytes) indicates a shallow proximal environment under fluvio-deltaic influx (Lister and Batten, 1988; Melia, 1984; Tahoun et al., 2017). This is supported by the low relative abundance of dinoflagellate cysts (between 1.6% and 15.08%) and low species richness (between 1 and 12 species) (Fig. 7) decreasing from the distal to the proximal shelf (Dale, 1983; Wall et al., 1977).

In general, interval B characterizes a proximal continental shelf under high continental influx. It shows fluctuations from a coastal oxic to a marginal anoxic stagnant continental shelf. It differs from the

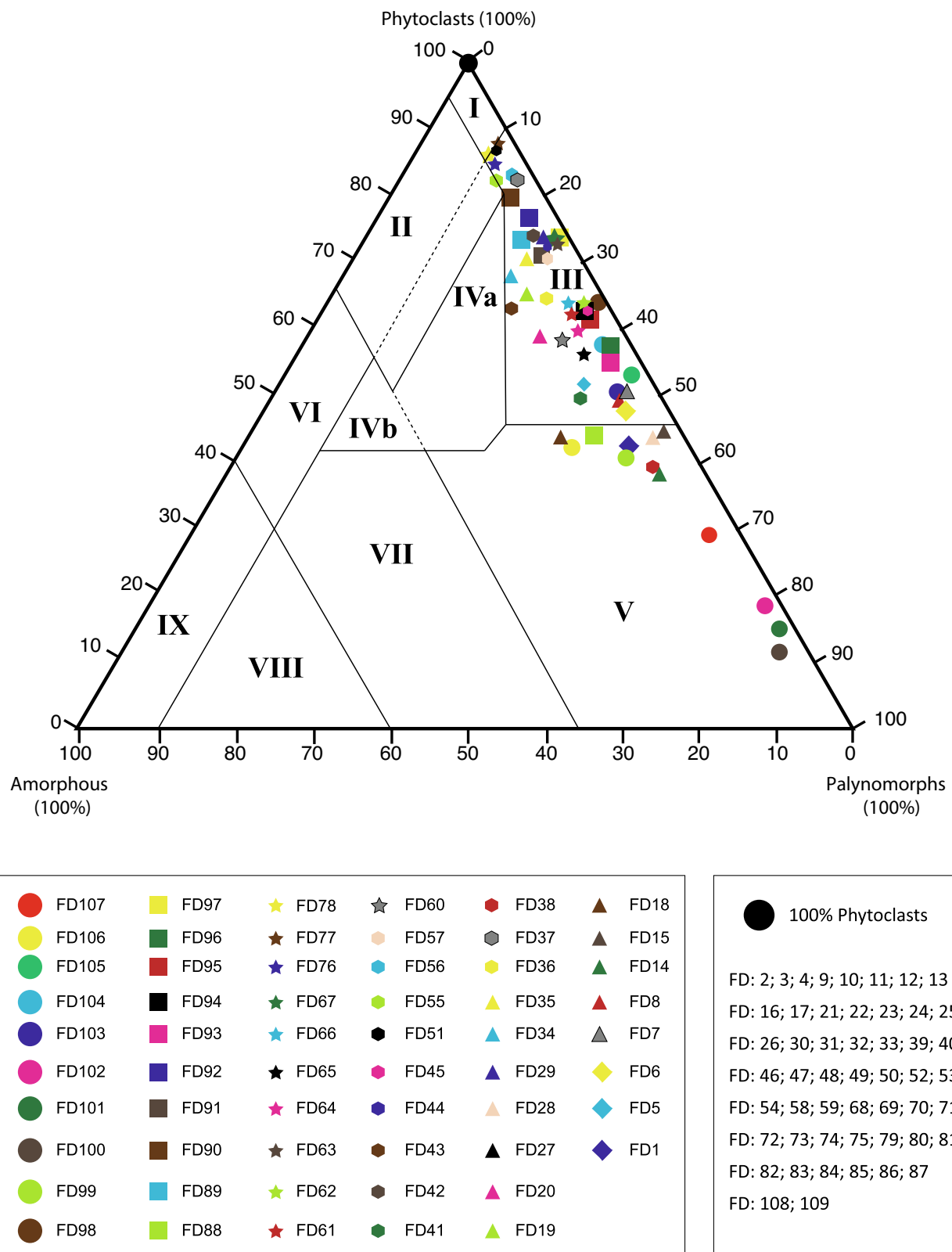


Fig. 8. Ternary MOA-Phytoclasts-Palynomorphs plot of the FD section (Tyson, 1993). Palynomorphs = spores + pollen + foraminifera + dinoflagellate cysts + Acritarchs + other marine algae; MOA = amorphous organic matter. Field I = type III kerogen; Field II = type III kerogen; Field III = type III or IV kerogen; Field IV = type III or II kerogen; Field V = type III or IV kerogen; Field VI = type II kerogen; Field VII = type II kerogen; Field VIII = type II or I kerogen; Field IX = type II or I kerogen.

paleoenvironment recognized in interval A by the absence of frequent marine incursions in the depositional environment.

- **Interval C:** defined between samples FD88 and FD109

In this 42 m thick interval, 13 samples are plotted in field III, 7 in field V and two samples in field I from the ternary diagram of Tyson (1993, 1995) (Fig. 8). The base of this interval (FD88), is characterized by the significant abundance of the marine fraction, especially dinoflagellate cysts which reach 45.33%, with species richness of 12 species. The S/D ratio recorded in interval C is between 0.16 and 0.80 (FD89, FD100).

The increase in abundance and species richness of dinoflagellate cysts is related to sea level rise (Batten, 1999; Tyson, 1993, 1995) and possibly a marine environment with normal salinity (Goodman, 1979; Habib et al., 1992; Lister and Batten, 1988; Mutterlose and Harding, 1987).

Proximal/coastal conditions are again recorded in samples FD89 to FD98, the latter samples belong to field III from the ternary diagram of Tyson (1993, 1995). They show a palynofacies dominated by M6b represented by translucent woody tissues and elongated wood fragments (Plate XII: 2), ranging between 11% and 79.33%. In these samples, spores and pollen grains show high relative abundances (between 70.6% and 80.6%), they are dominated by *Classopolis* and *Callialasporites* spp., which confirm the proximity of a terrestrial source. Marine fraction is represented by chitinous foraminifera (between 4.2% and 8.12%) and dinoflagellate cysts (between 12.91% and 25.11%) with a slight increase in species richness (10 species) compared to the previous interval B, which may imply a moderate deepening in the depositional environment (S/D ratio is between 0.70 and 0.80) (Fig. 7).

This depositional environment evolves to distal conditions manifested by increasing relative abundance of marine fraction reaching 84.1%. It is represented by dinoflagellate cysts, chitinous foraminiferal test linings and acritarchs. Dinoflagellate cysts range between 26.81% and 75.06% (Fig. 7), with an increase of species richness reaching 21 species in sample FD105. Species richness is largely applicable in the paleo-ecology of dinoflagellate cysts given that richness increases from the proximal to the distal shelf (Dale, 1983; Wall et al., 1977). Furthermore, its increase is a consequence of the appearance of new habitats for dinoflagellates due to marine transgressions (MacArthur and Wilson, 1967; Habib and Miller, 1989). Therefore, the eustatic rise observed in interval C may be correlated with the early Bathonian transgression (Hallam, 2001; Haq, 2018).

Previous paleoenvironmental conditions (proximal continental shelf/marginal), are restored in samples FD108 and FD109 (top of the FD section), plotted in field I and composed mainly of phytoclasts (MOx) (Fig. 8).

In general, interval C reflects a depositional environment with fluctuating conditions from a distal continental shelf to a proximal continental shelf/coastal. The base corresponds to a distal continental shelf with evidence of a marine incursion (probably late Bajocian marine transgression and two subsequent transgressions in the early Bathonian.) The restoration of proximal/marginal conditions is recorded in samples from the top of the studied section.

4.3. Biostratigraphical synthesis

In Morocco, palynological studies on Bajocian–Bathonian age are rare compared to those carried out in the Subboreal realm, particularly in northwest Europe. Most of them were carried out in the Guercif basin in northeast Morocco by Hssaida (1990, 1995), (Hssaida and Morzadec-Kerfourn, 1993, Hssaida et al., 2017). These authors dated sections from Bathonian-Oxfordian by dinoflagellate cysts. The biostratigraphy of the late Bajocian analyzed by dinoflagellate cysts has not been studied before.

Upper Bajocian-Lower Bathonian dinoflagellate cyst associations recognized in the Skoura syncline (Middle Atlas, Morocco) show

similarities with those recorded in northwest Europe by Riding and Thomas (1992), Riding (1994), Feist-Burkhardt and Monteil (1997), Poulsen and Riding (2003), Wiggan et al. (2017). They show similarities also with almost all the taxa recorded in the Tethyan realm by Conway (1990), Smelror (1993), El Beialy and Ibrahim (1997), Mafi et al. (2013). Principle resemblance includes the presence of *Durotrigia daveyi* in the basal late Bajocian, the presence of *Cribroperidinium crispum* and *Meiourogonyaulax valensii* in the late Bajocian. The latter species is found with *Dichadogonyaulax sellwoodii*, *Ctenidodinium combazii*, *Rhynchodiniopsis cladophora*, *Korystocysta pachyderma*, *Trichodinium scarburghense* characterizing the late Bajocian–early Bathonian; and finally, *Cribroperidinium venustum*, *Meiourogonyaulax reticulata* and *Aldorfia aldorfensis*, for the early Bathonian (Table 1).

The abundance of dinoflagellate cyst assemblages reported in northwest Europe throughout the late Bajocian–early Bathonian interval is related to the major two radiations recognized during the Bajocian (Fensome, 1996; Feist-Burkhardt and Monteil, 1997; Feist-Burkhardt and Gotz, 2016; Wiggan et al., 2017). These radiations coincide with significant and widespread increases in sea level (Wiggan et al., 2017). The first dinoflagellate evolutionary radiation is in the transition from the *S. Humphriesianum* Zone to the *S. Niortense* Zone. The second radiation takes place in the late Bajocian (P. Parkinsoni Zone)–early Bathonian (Z. Zigzag Zone) with a markedly more diverse assemblage. The latter phenomenon has been recorded in the FD section.

The proliferation and the abundance of Gonyaulacaceae is another similar event recorded both in the northwest of Europe (Fensome et al., 1996) and Skoura syncline (Morocco). Gonyaulacoid dinoflagellate cysts having multi-plate precingular and epicystal archeopyle such as *Ctenidodinium*, *Dissiliodinium*, *Durotrigia* and *Wanaea* were been remarkably abundant during the Bajocian (Feist-Burkhardt and Monteil, 1997 and 2001). This is confirmed in the FD section by the high relative abundance of *Dissiliodinium* and *Ctenidodinium* genus.

Despite the similarity between dinoflagellate cyst associations of both the Tethyan and the Subboreal realms during the late Bajocian–early Bathonian, some differences were noted in Moroccan deposits:

- *Meiourogonyaulax valensii* proliferates in sample FD99 (reaching 38.09%) just below the late Bajocian–early Bathonian transition.
- *Ctenidodinium cornigerum* is omnipresent during the late Bajocian (between samples FD1 and FD100), with two successive acmes in samples FD28 and FD38 (60% and 54.83% respectively).
- *Ctenidodinium combazii* is abundant in northwest Europe deposits (Riding and Thomas, 1992; Riding and Thomas, 1997; Wiggan et al., 2018). However, its presence is rather rare in the Tethyan realm (Hssaida, 1990, 1995; Jaydawi et al., 2016) and in some localities from northwest Europe, such as in England (Riding et al., 1991). Its absence or rarity may be due to its ecological preferences. *Ctenidodinium combazii* is stenohaline, preferring offshore marine environment under stable conditions (Riding et al., 1985, 1991). Other taxa, such as *Ctenidodinium sellwoodii*, *Korystocysta gochtii* and *Dissiliodinium* spp. are abundant in restricted conditions and tolerate variation in deposition parameters (Riding et al., 1985; Riding et al., 1991). The omnipresence of these taxa in the FD section in association with *Ctenidodinium cornigerum* indicates unstable conditions.

4.4. Palaeoenvironmental synthesis

The quantitative analysis of 109 samples from the late Bajocian–early Bathonian FD section allowed us to reconstitute the paleoenvironment's evolution during this time interval.

Thus, the late Bajocian depositional environment (intervals A and B), corresponds to a proximal continental shelf with a significant continental influx. The depositional environment shows oscillations between a proximal/coastal and marginal/stagnant environment.

The interval A (between the base of the section and sample FD38) shows repetitive marine incursions in the depositional environment,

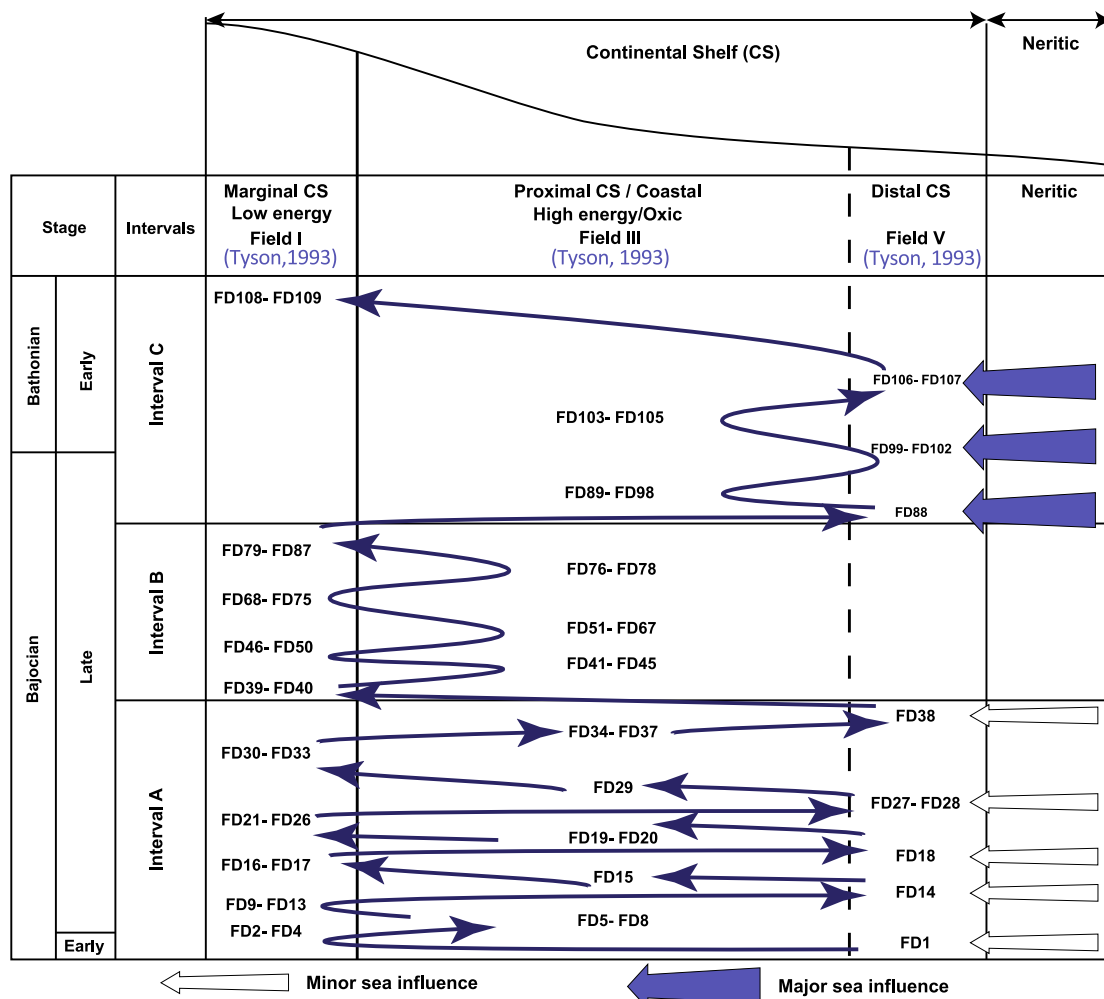


Fig. 9. Paleoenvironmental reconstruction of the FD section of the Skoura syncline (Middle Atlas, Morocco).

in contrast, in interval B (recognized between FD39 and FD87), marine pulsations are never detected. The continental elements composed of phytoclasts, spores and pollen grains still dominant in the two intervals. The low relative abundance of the amorphous organic matter (AOM) is related to the proximal/littoral depositional environment nature (field III samples) with high energy, most of which are winnowed leaving only small amounts of organic matter.

The sporadic appearance of algae (prasinophytes) indicates environmental stress due to lower salinity than normal (Batten, 1999; Lister and Batten, 1988). This is a characteristic of proximal environments close to fluvio-deltaic systems. This proximal coastal setting would be consistent with the dominance of terrestrial plant debris (Mob) and low diversity of dinoflagellate cysts related to the stressful conditions within an unfavorable environment, often with unstable salinities (Gorin and Steffen, 1991; Leckie et al., 1992; Tyson, 1995). This is supported by the presence of *Dissiliiodinium* spp. considered as ubiquitous, which indicates tolerance to restricted conditions, higher adaptation to paleoenvironmental variations (Riding et al., 1985; Riding et al., 1991) and low depths (Correia et al., 2018).

These findings indicate probably moderate rise and decrease of sea level during the late Bajocian with unstable, shallow paleoenvironment. The latter corresponds to a proximal continental shelf, sometimes highly agitated and often marginal stagnant.

At the top of the late Bajocian deposits (FD88), just below the late Bajocian-early Bathonian boundary, a significant marine pulsation or transgression, is recorded in the studied sediments inferred from the

high relative abundance of marine fraction dominated by dinoflagellate cysts (45.33%). This peak probably corresponds to the last Bajocian maximum flooding surface (MFS).

The environment evolves subsequently to a proximal/coastal environment (samples FD89 to FD98, plotted in field III) (Figs. 8 and 9), with a continued dominance of the terrestrial fraction (Mob, spores and pollen grains) in association with a moderate relative abundance of dinoflagellate cysts (between 12.91% and 25.11%).

The samples FD99, FD100, FD101, FD102, FD106 and FD107 plotted in field V (Figs. 8 and 9) enable us to identify the rise in sea level based on increasing dinoflagellate cysts abundance supported by an increase of species richness. This could be correlated with the late Bajocian and early Bathonian transition (*Parkinsonia parkinsoni* and *Ziggiceras zigzag*) that shows high species richness either in Germany (Mantle and Riding, 2012; Wigan et al., 2017) or in Portugal (Correia et al., 2018). This rising sea level may coincides with the Bathonian eustatic rise (Haq, 2018).

5. Conclusion

This work is the first palynological analysis based on dinoflagellate cysts of the Middle Jurassic marine formations carried out in the Tethyan Atlasic domain from Morocco. Although this work provides chronostratigraphic details on the geological deposits of the Bajocian-Bathonian transition, it provides valuable and complementary

information to those provided in similar works in the south Tethyan margin (Libya and Egypt).

In the Middle Atlas, rich dinoflagellate cyst assemblages have been noted from 109 samples of marls and limestones comprising 68 taxa including worldwide high-resolution stratigraphic marker taxa. Two association biozones are defined for the late Bajocian–early Bathonian interval. The *Cribroperidinium crispum*–*Ctenidodinium cornigerum* (CC/CC) biozone is defined between the base of the Recifa Formation (Upper Bajocian) and the Ich-Timellaline / Bou Akrabene Formation (Upper Bajocian–Lower Bathonian). The second association biozone of *Ctenidodinium combazii* and *Dichadogonyaulax sellwoodii* (CC/DS) corresponds to the last interval of the FD section (top of the Ich-Timellaline / Bou Akrabene Formation and the base of the El Mers I Formation). These two biozones were correlated with the late Bajocian–early Bathonian biozones defined in the Sub-Boreal (NW Europe), Tethyan and Australian domains. High similarity of associations between the Moroccan Middle Atlas, the Tethyan and the Sub-Boreal domains has been noted.

Quantitative analysis of organic matter components and palynofacies analysis has allowed the reconstruction of paleoenvironmental evolution. Five sea level increases have been recorded during the late Bajocian and one more during the early Bathonian.

With this contribution and considering that the studied section is very well exposed and easily accessible, it could be considered, in future works, a candidate type section for the southwestern part of the Tethyan domain.

Data availability

No data was used for the research described in the article.

Declaration of Competing Interest

The authors declare that they have no known competing financial interests or personal relationships that could have appeared to influence the work reported in this paper.

Acknowledgements

The authors would like to thank the Editor-in-Chief Prof. Dr. Henk Brinkhuis, reviewer Sander Houben and the anonymous reviewer for their positive and constructive comments which improved the quality of the manuscript.

Appendix A. Appendix 1

An alphabetical list of palynomorphs identified in the Ich Timellaline/ Bou Akrabene Formation of the Skoura Syncline and discussed in the text and/or Table 1. References to the dinoflagellate cyst author citations can be found in Fensome and Williams (2004). Selected dinoflagellate cysts, spores and pollen grains are illustrated in Plates I–XII.

A.1. Dinoflagellate cysts

Aldorfia aldorfensis (Gocht, 1970b) Stover and Evitt, 1978.
Ambonosphaera? cf. *staffinensis* (Gitmez, 1970).
Batiacasphaera spp. (Drugg, 1970b) Emend: Morgan, 1975, Dörhöfer and Davies, 1980.
Bradleyella Adela (Fenton et al., 1980) Woollam, 1983.
Cassiculosphaeridium spp. (Davey, 1969a) Courtinat 1989.
Cavatodissiliodinium spp. (Feist-Burkhardt and Monteil, 2001).
Cribroperidinium cf. *crispum* (Wetzel, 1967a) Woollam and Riding, 1983, Emend: Sarjeant, 1980b, Fenton, 1981.

Cribroperidinium crispum (Wetzel, 1967a) Woollam and Riding, 1983, Emend: Sarjeant, 1980b, Fenton, 1981.

Cribroperidinium venustum (Klement, 1960) Poulsen, 1996.
Ctenidodinium combazii (Dupin, 1968).
Ctenidodinium continuum (Gocht, 1970b).
Ctenidodinium cornigerum (Valensi, 1953) Jan du Chêne et al., 1985b, Emend: Jan du Chêne et al., 1985b.

Ctenidodinium ornatum (Eisenack, 1935) Deflandre, 1939a.
Ctenidodinium spp. (Deflandre, 1939a) Emend: Sarjeant, 1966b, Sarjeant, 1975a, Woollam, 1983, Benson, 1985.
Ctenidodinium sellwoodii (Sarjeant, 1975a) Stover and Evitt, 1978, Sarjeant, 1975a.

Dissiliodinium giganteum (Feist-Burkhardt, 1990).
Dissiliodinium minimum (Feist-Burkhardt and Monteil, 2001).
Dissiliodinium omentum (Feist-Burkhardt and Monteil, 2001).
Dissiliodinium primum (Feist-Burkhardt and Monteil, 2001).
Dissiliodinium spp. (Drugg, 1978) Emend: Bailey and Partington, 1991, Feist-Burkhardt and Monteil, 2001.

Dissiliodinium sp1. (Drugg, 1978) Emend: Bailey and Partington, 1991, Feist-Burkhardt and Monteil, 2001.

Dissiliodinium sp2. (Drugg, 1978) Emend: Bailey and Partington, 1991, Feist-Burkhardt and Monteil, 2001.

Durotrigia daveyi (Bailey, 1987).
Ellipsoidicty whole group (Klement, 1960).
Endoscrinium asymmetricum (Riding, 1987a).
Endoscrinium spp. (Klement, 1960) Vozzhenikova, 1967.
Epiplosphaera gochtii (Ellipsoidicty whole group) (Fensome, 1979).
Epiplosphaera spp. (Klement, 1960) Emend: Brenner, 1988.
Escharisphaeridida spp. (Erkmen and Sarjeant, 1980).
Gonyaulacysta eisenackii (Deflandre, 1939a) Górká, 1965; Emend: Sarjeant, 1982b.

Gonyaulacysta jurassica (Deflandre, 1939a) Norris and Sarjeant, 1965, Emend: Sarjeant, 1982b.

Gonyaulacysta jurassica subsp. *Alecto* (Sarjeant, 1982b).
Gonyaulacysta jurassica var. *longicornis*, (Deflandre, 1939a) Lentin and Williams, 1973.

Gonyaulacysta pectinigera (Gocht, 1970b) Fensome, 1979, Emend: Fensome, 1979.

Kallosphaeridium spp. (de Coninck, 1969) Emend: Jan du Chêne et al., 1985.

Kalyptea stegasta (Sarjeant, 1961a) Wiggins, 1975.
Korystocysta gochtii (Sarjeant, 1976a) Woollam, 1983.
Korystocysta pachyderma (Deflandre, 1939a) Woollam, 1983.
Korystocysta sp1. (Woollam, 1983) Emend: Benson, 1985.
Korystocysta spp. (Woollam, 1983) Emend: Benson, 1985, Courtinat 1989.

Leptodinium spp. (Klement, 1960) Emend: Sarjeant, 1966b, Wall, 1967 and Sarjeant, 1969.

Meiourgonyaaulax caytonensis, (Sarjeant, 1959) Sarjeant, 1969.
Meiourgonyaaulax cf. *caytonensis* (Sarjeant, 1959) Sarjeant, 1969.
Meiourgonyaaulax cf. *deflandrei* (Sarjeant, 1968).
Meiourgonyaaulax cf. *valensi* (Valensi, 1953) Sarjeant, 1966b.
Meiourgonyaaulax *reticulata* (Dodekova, 1975).
Meiourgonyaaulax sp1. (Sarjeant, 1966b) Gocht, 1975b and Williams et al., 1993.

Meiourgonyaaulax sp2. (Sarjeant, 1966b) Gocht 1975b; and Williams et al., 1993.

Meiourgonyaaulax sp3. (Sarjeant, 1966b) Gocht 1975b; and Williams et al., 1993.

Meiourgonyaaulax spp. (Sarjeant, 1966b) Gocht 1975b, and Williams et al., 1993.

Meiourgonyaaulax valensi, (Sarjeant, 1966b) Valensi, 1953, Sarjeant, 1966b.

Pareodinia ceratophora (Deflandre, 1947d) Emend: Gocht, 1970b.

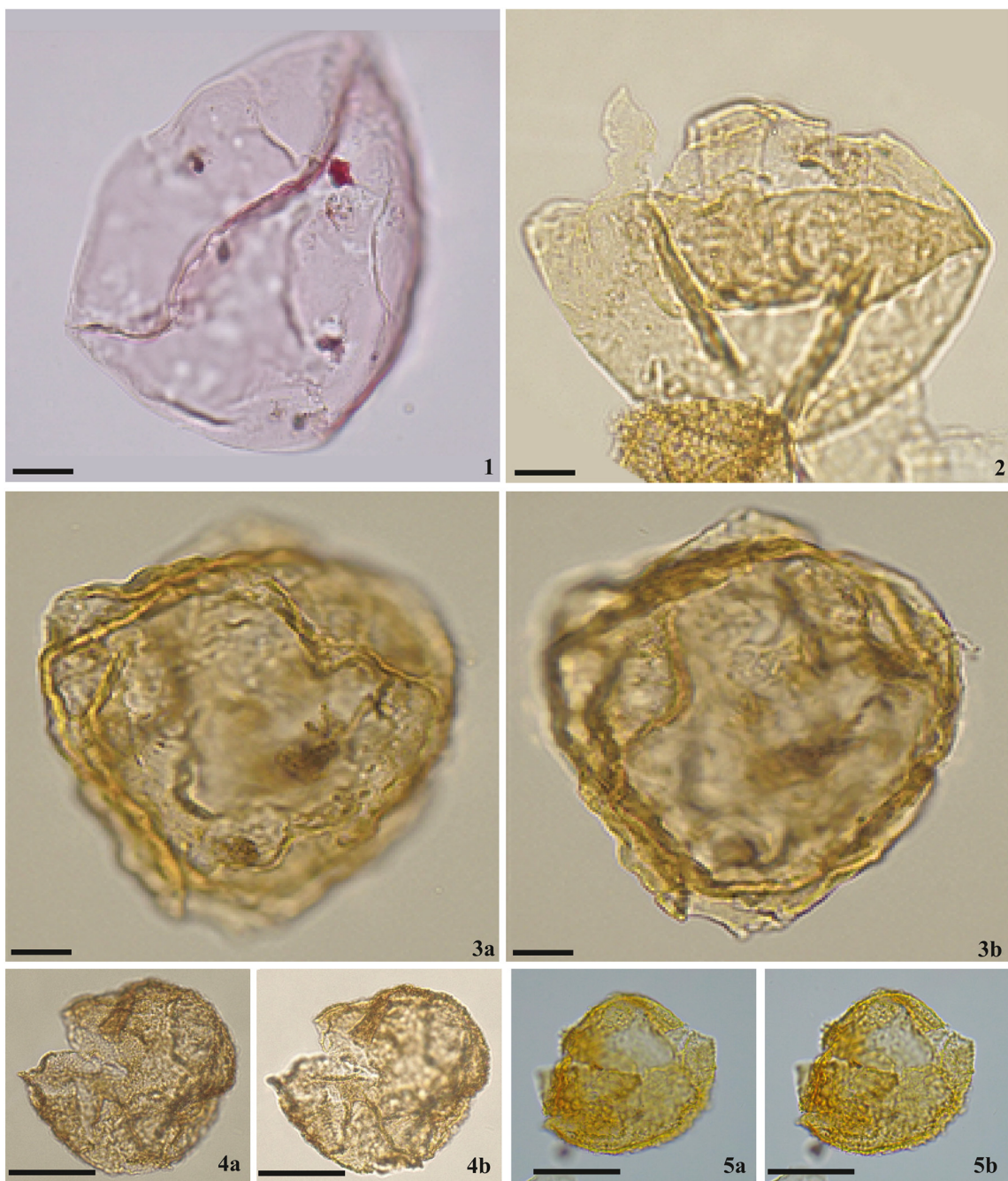


Plate I. Photo micrographs of dinoflagellate cysts from the late Bajocian to early Bathonian of the FD section, Skoura syncline, Middle Atlas, Morocco. Each specimen identified by sample, slide number and England finder coordinates.

Scale bar in Figure represents 20 µm.

1. *Dissiliiodinium giganteum* Feist-Burkhardt, 1990, Sample FD36, Slide a, X47/1. This specimen represents a perforated wall exactly like the one found in the Lower Bajocian, Laeviuscula zone, in SW-Germany par Feist-Burkhardt, 1992).

2. *Dissiliiodinium giganteum* Feist-Burkhardt, 1990, Sample FD100, Slide a, R36/2.

3.a-b. *Dissiliiodinium giganteum* Feist-Burkhardt, 1990, Sample FD101, Slide a, J21/3. (This cyst presents a cavation probably it is a *Cavatodissiliiodinium*).

4a-b et 5.a-b. *Dissiliiodinium minimum* Feist-Burkhardt and Monteil, 2001, 4a and b: Sample FD101, Slide b, T56/57. 5a and 5b: Sample 100, Slide a, Y32/33.

Pareodinia, Deflandre (1947d) Emend: Gocht, 1970b, Johnson and Hills, 1973, Wiggins, 1975.

Rhynchodiniopsis cladophora (Deflandre, 1939a) Below, 1981a.

Rhynchodiniopsis regalis (Gocht, 1970b) Jan du Chêne et al., 1985b.

Rhynchodiniopsis spp. (Deflandre, 1935) Emend: Below, 1981a; Sarjeant, 1982b.

Sentusidinium rioultei (Sarjeant, 1968) Sarjeant and Stover, 1978; Emend: Courtinat, 1989.

Sentusidinium spp. (Sarjeant and Stover, 1978) Emend: Courtinat, 1989.

Sirmiodiniopsis orbis (Drugg, 1978).

Sirmiodiniopsis spp. (Drugg, 1978) Lentin and Williams 1981.

Tehamadinium spp. (Jan du Chêne et al., 1986b, Jan du Chêne et al. 1986a).

Trichodinium scarburghense (*Acanthaulax scarburghensis*), (Sarjeant, 1964).

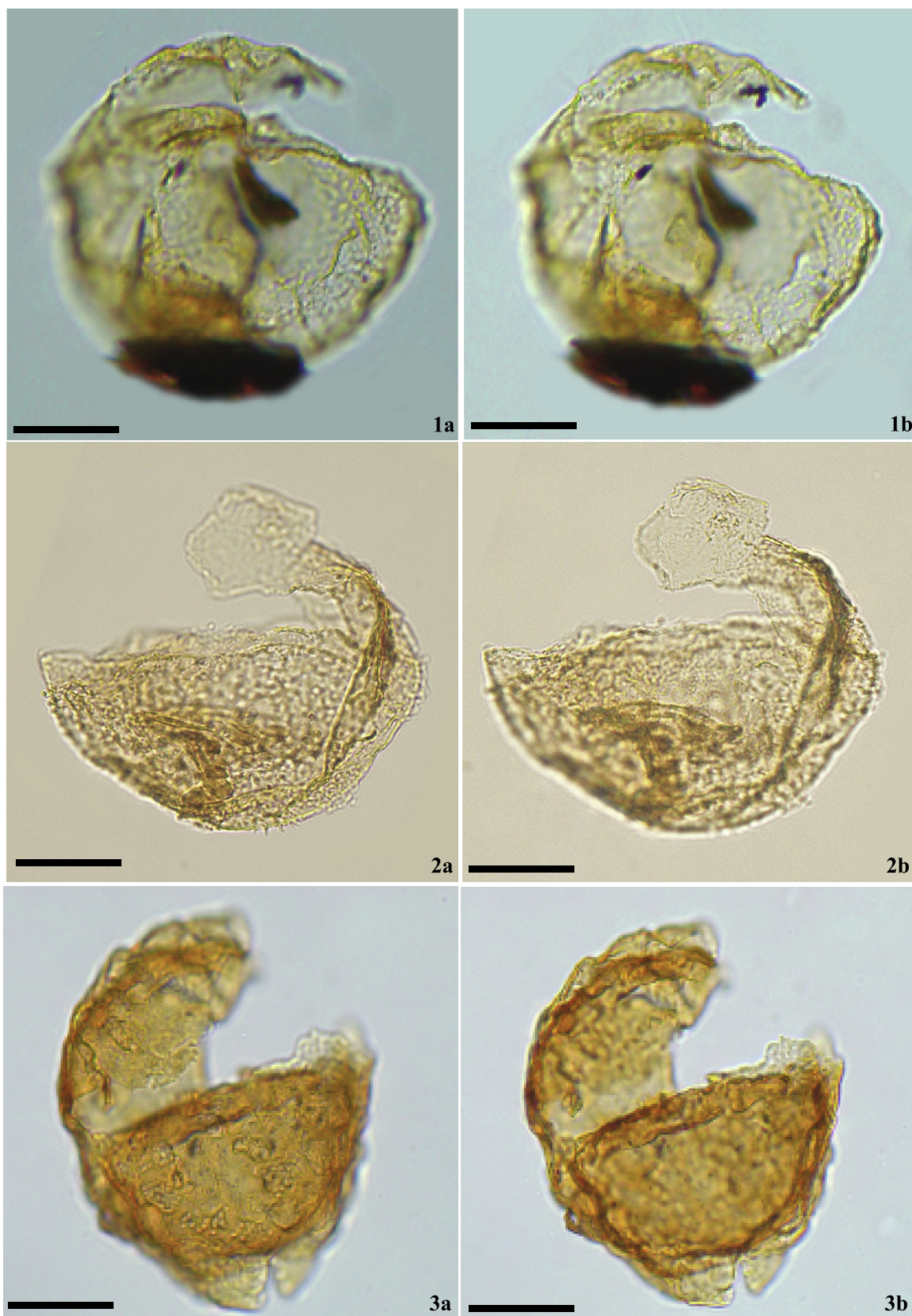


Plate II. Photo micrographs of dinoflagellate cysts from the upper Bajocian to Lower Bathonian in the (FD) section, Skoura syncline, Middle Atlas, Morocco. Each specimen identified by sample, slide number and England finder coordinates.

Scale bar in Figure represent 20 µm.

- 1.a. *Dissiliodinium omentum*, Feist-Burkhardt and Monteil, 2001. Sample FD8, Slide a, Q37. High focus on the dorsal face, focus on the 3" and 4" paraplate.
- 1.b. *Dissiliodinium omentum*, Feist-Burkhardt and Monteil, 2001. Sample FD8, Slide a, Q37. high focus on the dorsal face. The two intermediate paraplates are visible.
- 2.a. *Dissiliodinium primum*, Feist-Burkhardt and Monteil, 2001. Sample FD100, Slide a, P50, paratabulation was only expressed by the paracingulum. Epicyst is attached to the hypocyst. High focus on the paracingulum, wall is scabrate to granulate.
- 2.b. *Dissiliodinium primum*, Feist-Burkhardt and Monteil, 2001. Sample FD100, Slide a, P50. high focus on one anterior intercalary paraplate.
- 3.a-b. *Cavatodissiliodinium* spp., Feist-Burkhardt and Monteil, 2001, Sample FD101, Slide b, V44/3.

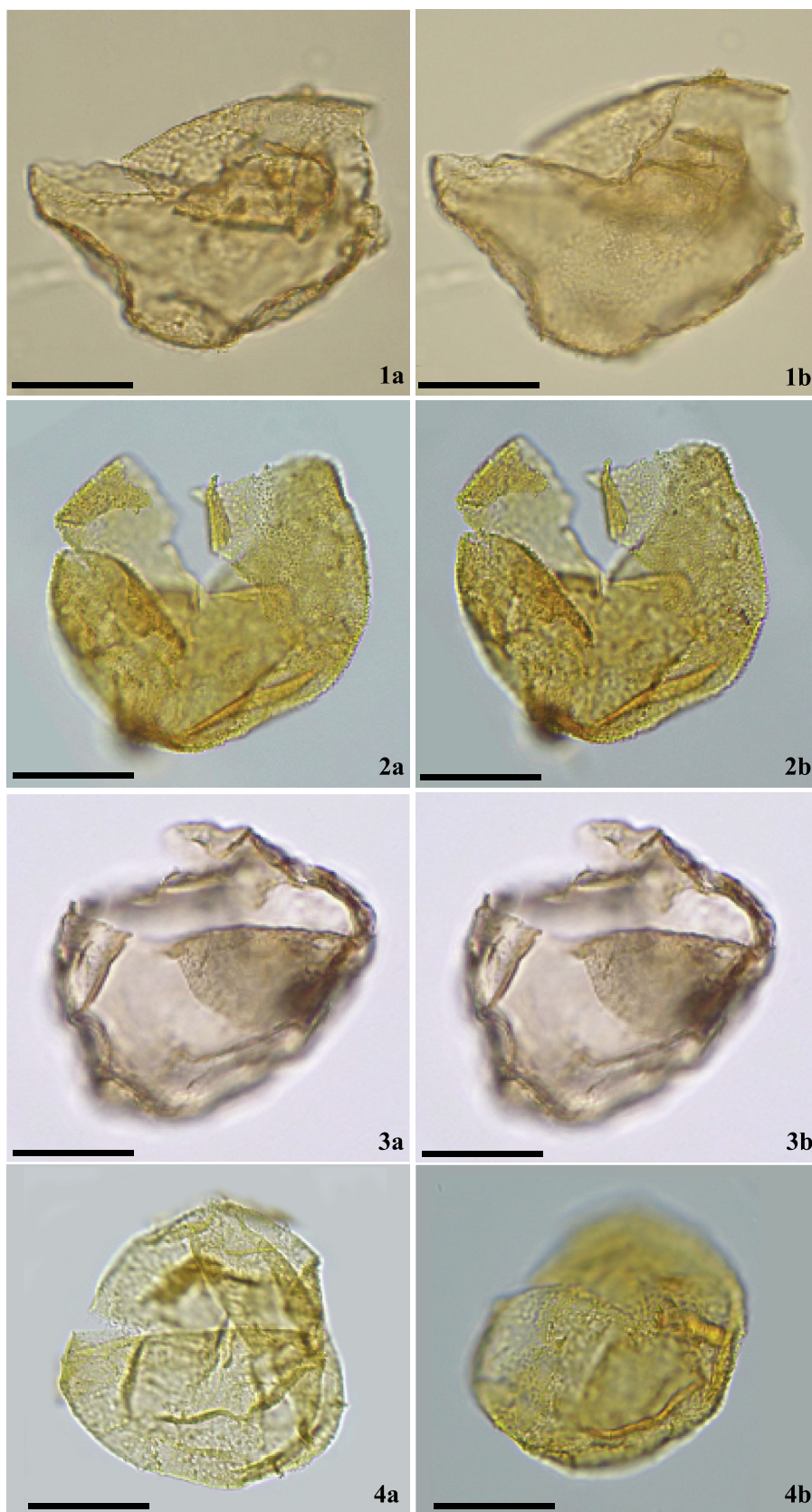


Plate III. Photo micrographs of dinoflagellate cysts from the upper Bajocian to Lower Bathonian in the (FD) section, Skoura syncline, Middle Atlas, Morocco. Each specimen identified by sample, slide number and England finder coordinates.

Scale bar in Figure represent 20 µm.

1.a. *Dissiliodium* sp1., Drugg, 1978. Sample FD101, Slide a, X32. reticulated wall and absence of paratabulation.

1.b. *Dissiliodium* sp1., Drugg, 1978. Sample FD101, Slide a, X32. Focus on the apical protrusion.

2. a-b. *Dissiliodinium primum*, Feist-Burkhardt and Monteil, 2001. Sample FD100, Slide a, N27/1, Focus on the surface densely granulated. Paratabulation not visible.

3.a-b. *Dissiliodinium* spp., Sample FD07, Slide b, O52/2, presence of the two intercalary anterior paraplate.

4.a. *Dissiliodinium* sp. 2., Drugg, 1978. Sample FD100, slide a, R46/1, the epicyst is always connected to the hypocyst.

4.b. *Dissiliodinium* sp. 2., Drugg, 1978. Sample FD100, slide a, Y39, wall finely granulated and absence of the Intercalary paraplate.

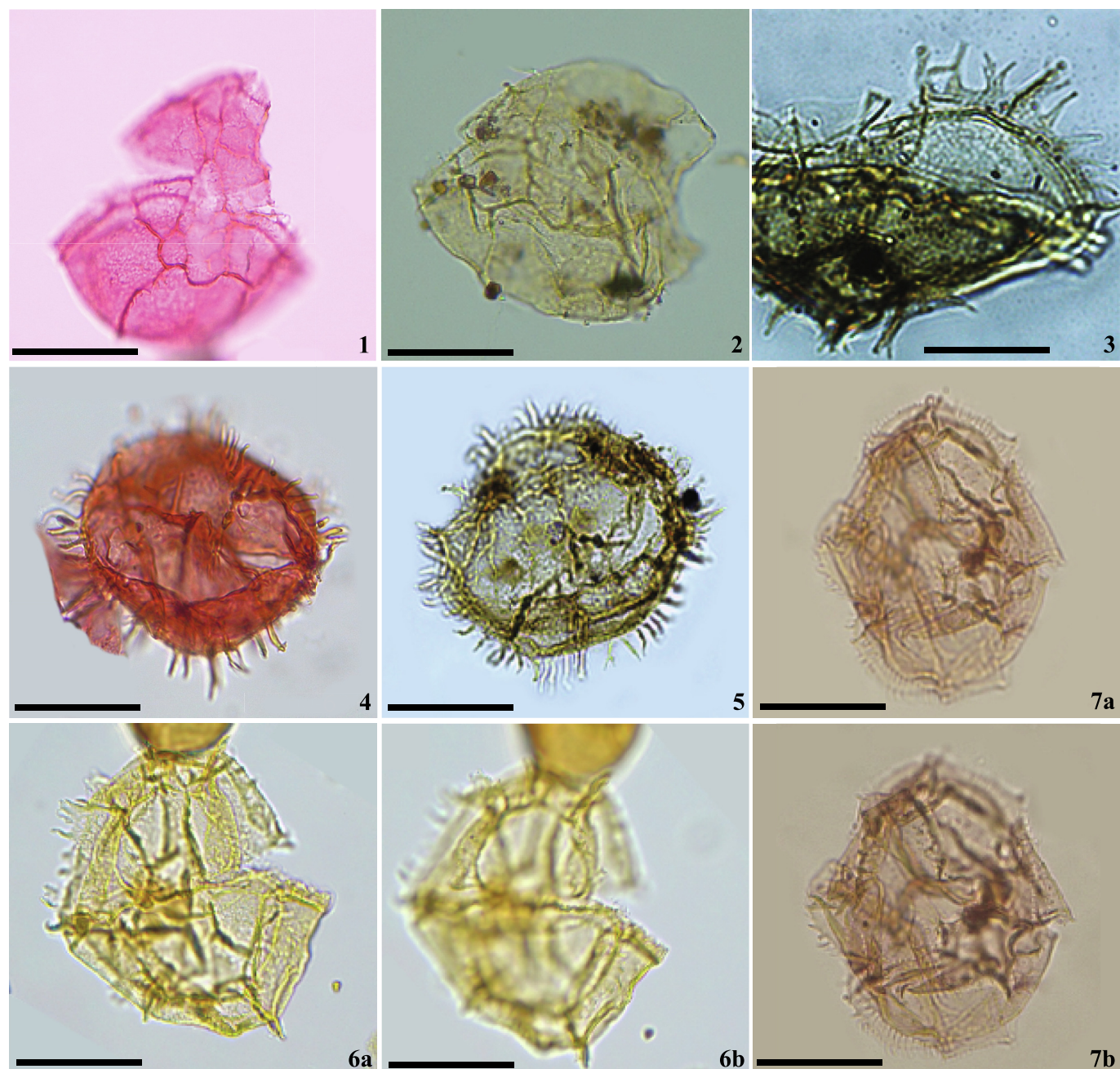


Plate IV. Photo micrographs of dinoflagellate cysts from the upper Bajocian to Lower Bathonian in the (FD) section, Skoura syncline, Middle Atlas, Morocco. Each specimen identified by sample, slide number and England finder coordinates.

Scale bar in Figure represent 20 µm.

1. *Dichadogonyaulax sellwoodii*, Sarjeant, 1975a, Lentin and Williams (1993). Sample FD28, slide b, J23.
2. *Dichadogonyaulax sellwoodii*, Sarjeant, 1975a, sample FD28, slide a, M41.
3. *Ctenidodinium combazii*, Dupin, 1968, sample FD100, slide a, Q21/3.
4. *Ctenidodinium cornigerum*, Valensi, 1953, Emend : Jan du Chêne et al., 1985b. Sample FD36, slide b, H21/2.
5. *Ctenidodinium cornigerum*, Valensi, 1953, Emend : Jan du Chêne et al., 1985b. Sample FD38, slide a, K41/1.
- 6.a-b. *Ctenidodinium ornatum*, Eisenack, 1935, sample FD107, slide a, H23.
- 7a-b. *Ctenidodinium continuum*, Gocht, 1970b, sample FD105, slide b, R18/2.

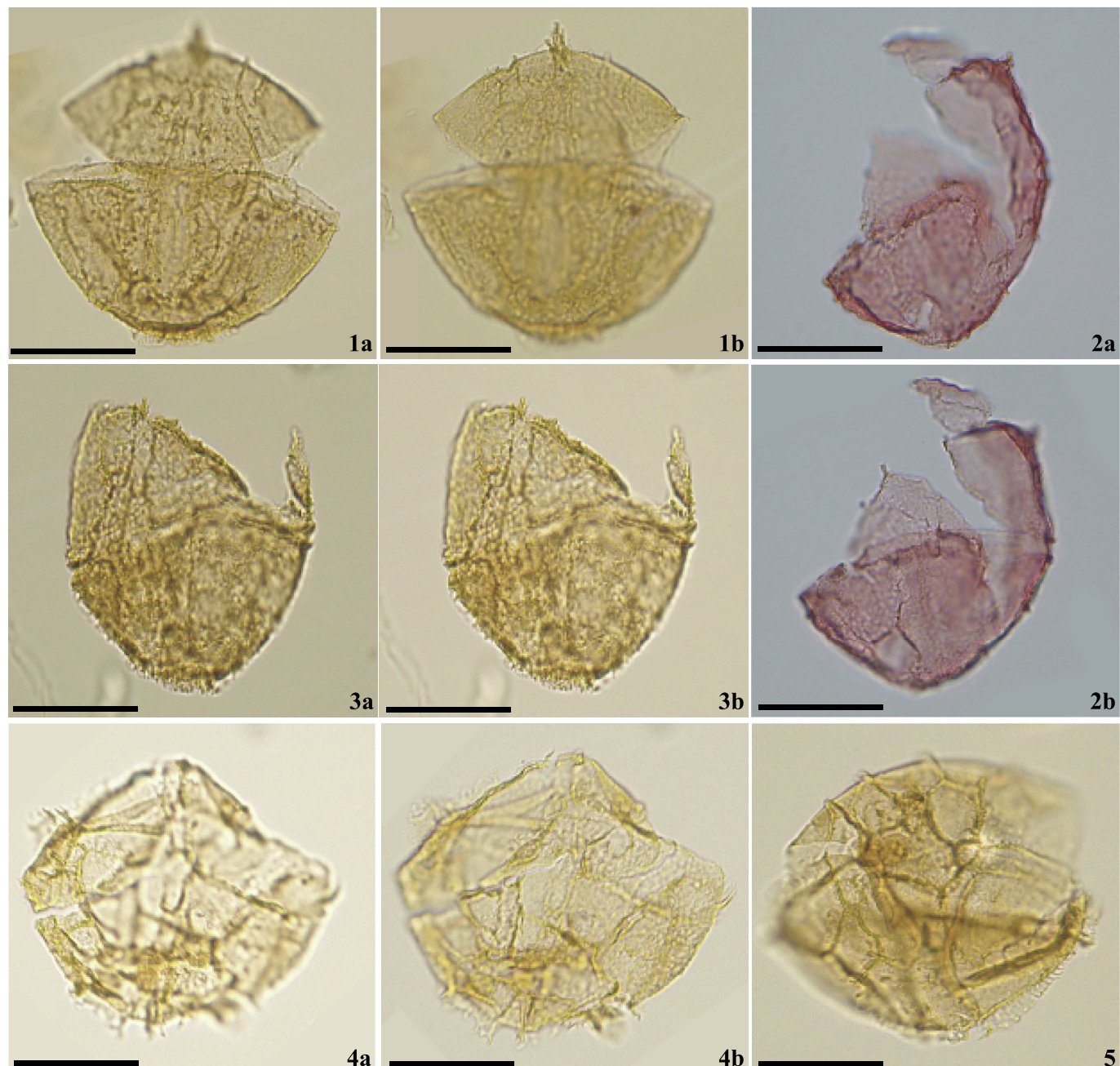


Plate V. All Photo micrographs of dinoflagellate cysts from the upper Bajocian to Lower Bathonian in (FD) section, Skoura syncline, Middle Atlas, Morocco. Each specimen identified by sample, slide number and England finder coordinates.

Scale bar in Figure represent 20 µm.

1.a-b. *Korystocysta pachyderma*, Deflandre, 1939a, Woollam, 1983. Sample FD100, slide b, K36.

2.a-b. *Korystocysta gochtii*, Sarjeant, 1976a, Woollam, 1983. Sample FD43, slide b, N42/1.

3.a-b. *Korystocysta gochtii*, Sarjeant, 1976a, Woollam, 1983. Sample FD100, slide a, H27/4.

4.a-b. *Rhynchodiniopsis cladophora*, Deflandre, 1939a, Below, 1981a. Sample FD100, Slide a, M49/2.

5. *Ctenidodinium* spp., Deflandre, 1939a, sample FD100, Slide a, R41/2.

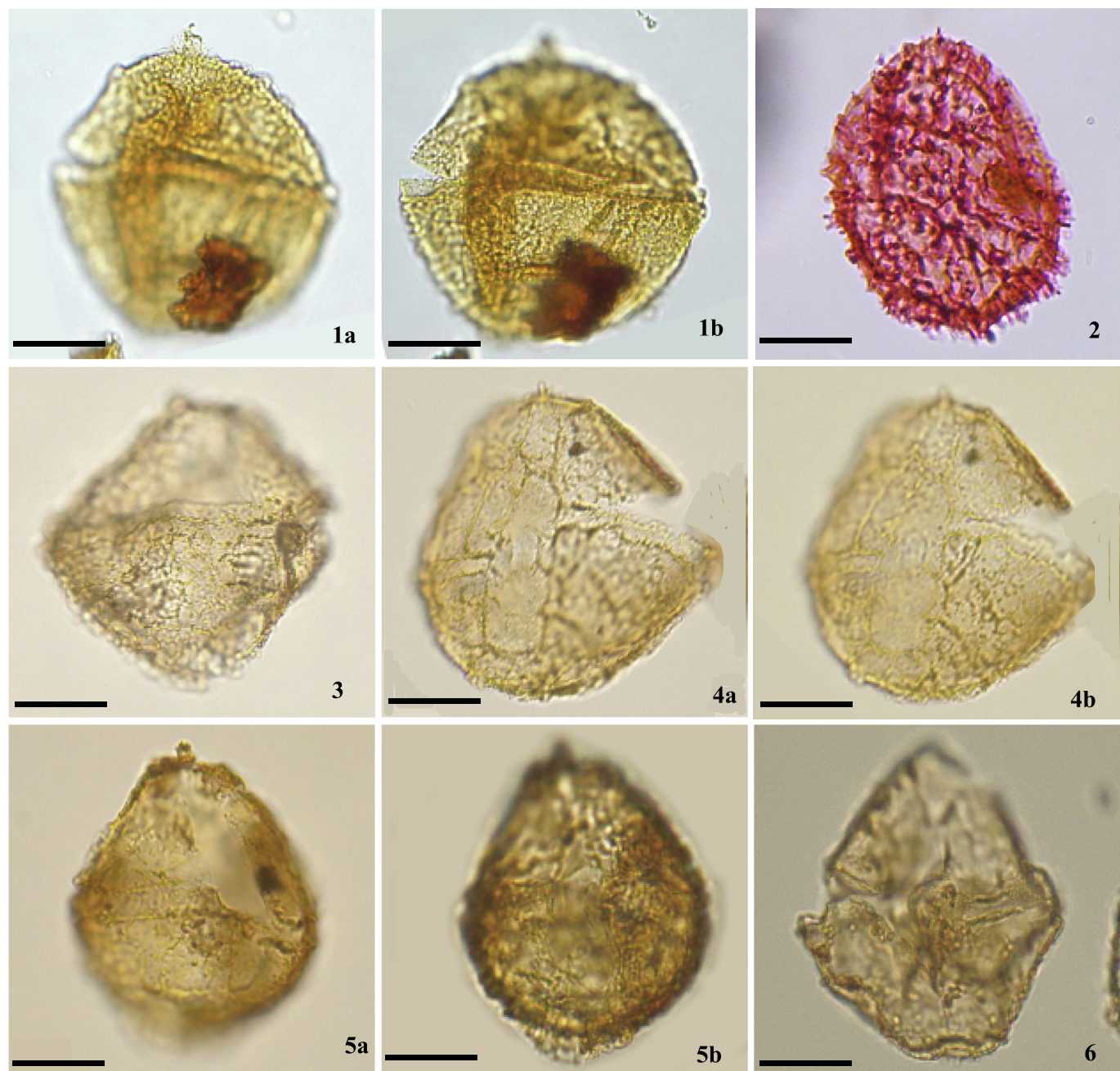


Plate VI. Photo micrographs of dinoflagellate cysts from the upper Bajocian to Lower Bathonian in the (FD) section, Skoura syncline, Middle Atlas, Morocco. Each specimen identified by sample, slide number and England finder coordinates.

Scale bar in Figure represent 20 µm.

1.a-b. *Trichodinium scarburghense*, Sarjeant, 1964b, Williams et al., 1993. Sample FD100, slide b, G25/3.

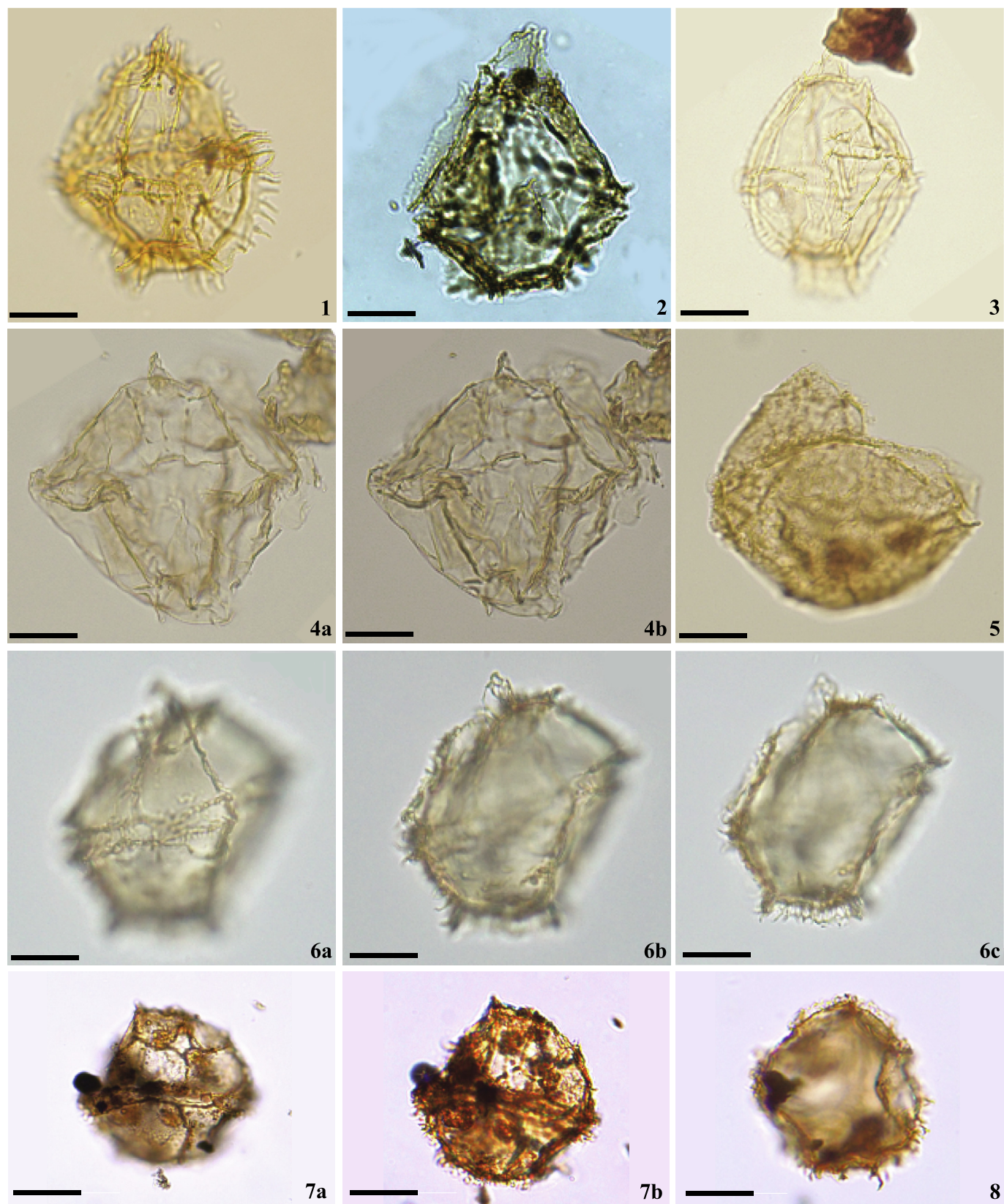
2. *Cribroperidinium venustum*, Klement, 1960, Poulsen, 1996. Sample FD100, slide a, N52/2.

3. *Cribroperidinium crispum*, Wetzel, 1967a, Emend: Sarjeant, 1980b, Fenton, 1981. Sample FD101, slide a, G49.

4.a-b. *Cribroperidinium crispum*, Wetzel, 1967a, Emend: Sarjeant, 1980b, Fenton, 1981. Sample FD100, slide b, O39/3.

5. *Aldorfia aldorvensis*, Gocht, 1970b, Stover and Evitt, 1978. Sample FD101, slide a, Q24/1.

6. *Willeidinium* spp., Feist-Burkhardt, 1995a, sample FD101, slide b, N57/4.



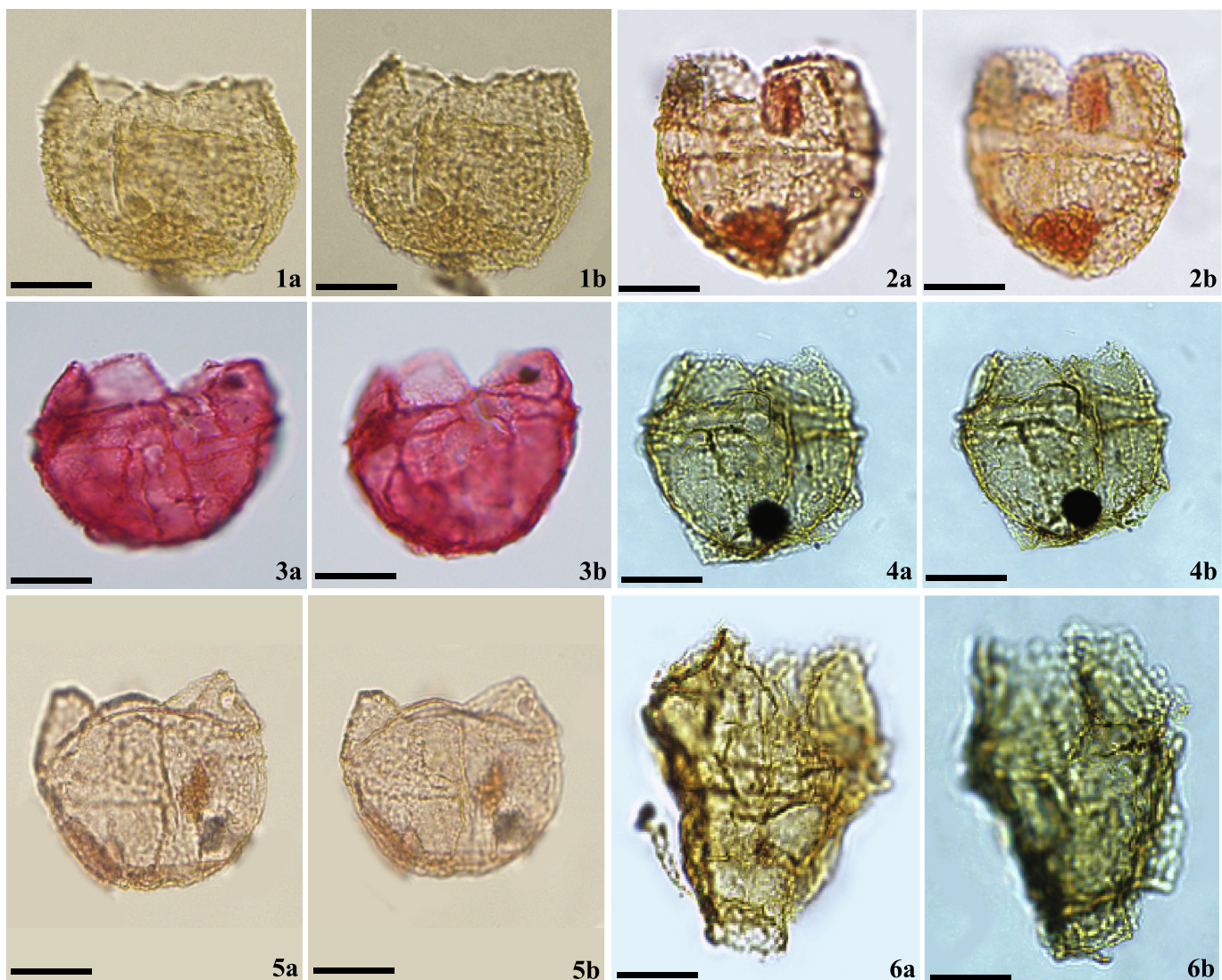


Plate VIII. Photo micrographs of dinoflagellate cysts from the upper Bajocian to Lower Bathonian in the (FD) section, Skoura syncline, Middle Atlas, Morocco. Each specimen identified by sample, slide number and England finder coordinates.

Scale bar in Figure represent 20 µm.

- 1.a-b. *Meiourogonyaulax caytonensis*, Sarjeant, 1959, Sarjeant, 1969. Sample FD100, slide b, H34/.
- 2.a-b. *Meiourogonyaulax reticulata*, Dodekova, 1975. Sample FD107, slide a, X54/55.
- 3.a-b. *Meiourogonyaulax caytonensis*, Sarjeant, 1959, Sarjeant, 1969. Sample FD102, slide a, S37/3.
- 4.a-b. *Meiourogonyaulax valensi*s, Sarjeant, 1966b, Sarjeant, 1966b. Sample FD90, slide a, Q34/3.
- 5.a-b. *Meiourogonyaulax cf. deflandrei*, Sarjeant, 1968, sample FD105, slide b, P48/3.
- 6.a. *Meiourogonyaulax valensi*s, Sarjeant, 1966b, Sarjeant, 1966b. Sample FD90, slide a, D42.
- 6.b. *Meiourogonyaulax valensi*s, Sarjeant, 1966b, Sarjeant, 1966b. Sample FD90, slide a, H43/44.

Plate VII. Photo micrographs of dinoflagellate cysts from the upper Bajocian to Lower Bathonian in the (FD) section, Skoura syncline, Middle Atlas, Morocco. Each specimen identified by sample, slide number and England finder coordinates.

Scale bar in Figure represent 20 µm.

1. *Gonyaulacysta pectinigera*, Gocht, 1970b, Emend: Fensome, 1979. Sample FD102, slide b, X23/4.
2. *Gonyaulacysta jurassica* subsp. *Alecta*, Deflandre, 1939a, sample FD105, slide a, V26.
3. *Tubotuberella dangeardii*, Sarjeant, 1968, Stover and Evitt, 1978. Sample FD100, slide a, W37/1.
- 4.a-b. *Endoscrinium asymmetricum*, Riding, 1987a, sample FD101, slide b, L50/2.
5. *Tehamadinium* spp., Jan du Chêne et al., 1986b, sample FD100, Z27/1.
- 6.a-b-c. *Rhynchodiniopsis regalis*, Gocht, 1970b, Jan du Chêne et al., 1985b. Sample FD101, slide b, G48.
- 7.a. *Durotrigia daveyi*, Bailey, 1987, sample FD01, slide a, H41. Focus on the 2 a paraplate.
- 7.b. *Durotrigia daveyi*, Bailey, 1987, sample FD01, slide a, H41.
8. *Durotrigia daveyi*, Bailey, 1987, sample FD01, slide a, U30/1, focus on the discontinuous parasutural ridges with isolated spines which are generally distally linked by thin, smooth trabeulae

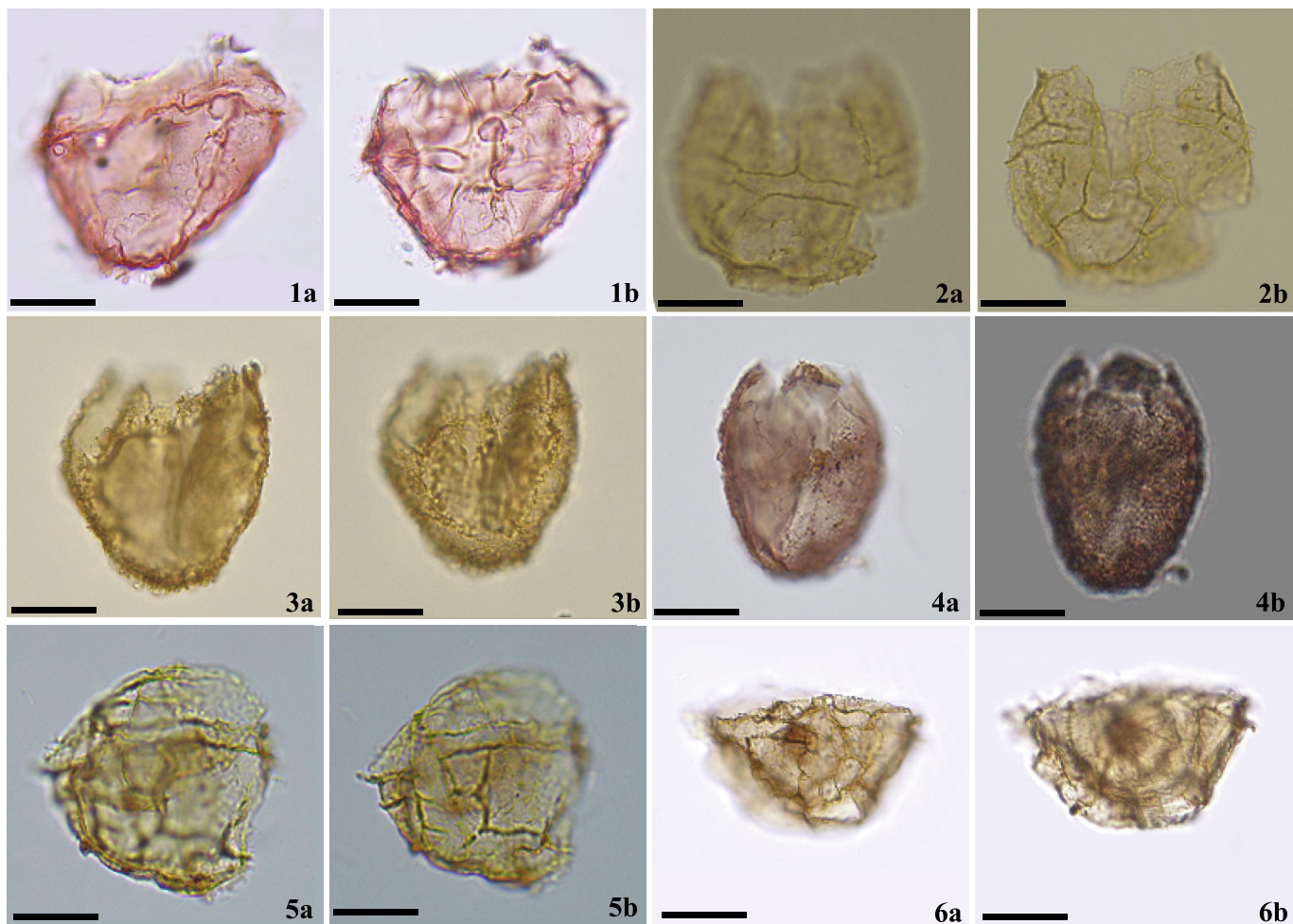


Plate IX. Photo micrographs of dinoflagellate cysts from the upper Bajocian to Lower Bathonian in the (FD) section, Skoura syncline, Middle Atlas, Morocco. Each specimen identified by sample, slide number and England finder coordinates.

Scale bar in Figure represent 20 µm.

- 1.a. *Meiourogonyaulax* sp1. Sarjeant, 1966b, sample FD105, slide a, U53/2, dorsal face, septa very cut.
- 1.b. *Meiourogonyaulax* sp1. Sarjeant, 1966b, sample FD105, slide a, U53/2, ventral face. Septa with processes. Vacuolated wall.
- 2.a-b. *Meiourogonyaulax* spp. Sarjeant, 1966b, sample FD100, slide b, C55/56.
- 3.a-b. *Meiourogonyaulax* sp2. Sarjeant, 1966b, sample FD101, slide a, S54/4. The wall ornamented by processes.
- 4.a. *Meiourogonyaulax* sp3. Sarjeant, 1966b, sample FD38, slide b, G36/4. Focus on the archeopyle.
- 4.b. *Meiourogonyaulax* sp3. Sarjeant, 1966b, sample FD38, slide b, G36/4. Focus on the microreticulated wall.
- 5.a-b. *Meiourogonyaulax* spp. Sarjeant, 1966b, sample FD08, slide b, D24/4.
6. a-b. *Ambo nosphaera* cf. *staffinensis*, Gitmez, 1970, sample FD105, slide a, Z25/26.

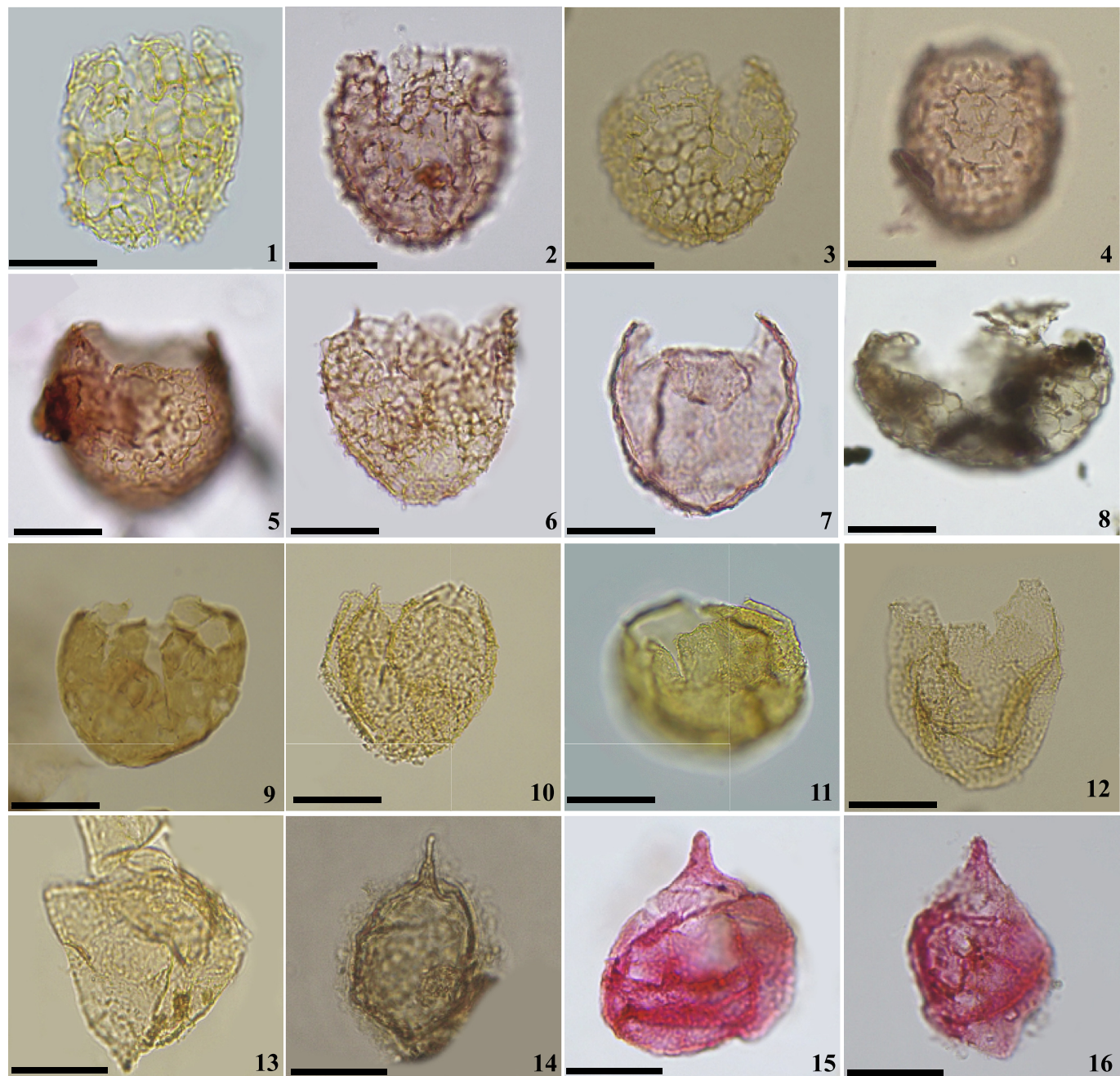
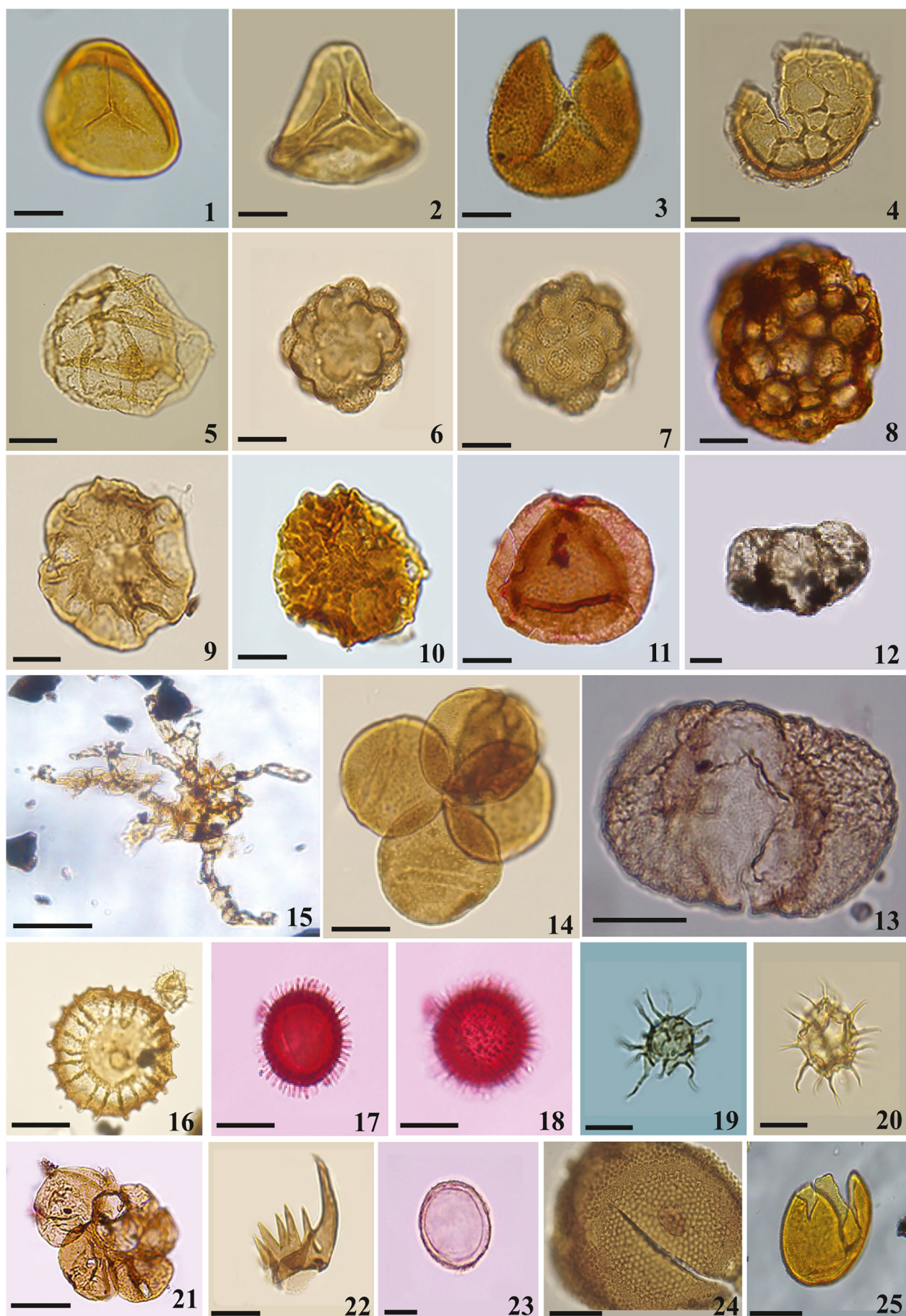


Plate X. Photo micrographs of dinoflagellate cysts from the upper Bajocian to Lower Bathonian in the Al Feddane (FD) section, Skoura syncline, Middle Atlas, Morocco. Each specimen identified by sample, slide number and England finder coordinates.

Scale bar in Figure represent 20 µm.

1. *Ellipsoidictyum cinctum*, Klement, 1960, sample FD100, slide a, U40/2.
2. *Epiplosphaera gochtii*, Fensome, 1979, sample FD105, slide b, L23/2.
3. *Valensiella ovulum*, Deflandre, 1947d, sample FD100, slide a, M37/1.
4. *Valensiella vermiculata*, Gocht, 1970b, sample FD105, slide a, O41/3.
5. *Valensiella vermiculata*, Gocht, 1970b, sample FD105, slide a, M26.
6. *Epiplosphaera gochtii*, Fensome, 1979, sample FD107, slide a, L40/2.
7. *Batiacasphaera* spp., Drugg, 1970b, sample FD43, slide b, E31/2.
8. *Cassiculosphaeridium* spp., Davey, 1969a, sample FD01, slide a, B40.
9. *Kallosphaeridium* spp., de Coninck, 1969, sample FD88, slide b, Z47.
10. *Sentusidinium rioultei*, Sarjeant, 1968, sample FD102, slide a, O45.
11. *Kallosphaeridium* spp., de Coninck, 1969, sample FD100, slide a, O26.
12. *Sentusidinium* spp., Sarjeant and Stover, 1978, sample FD100, slide b, V24/4.
13. *Wanaea acollaris*, Dodekova, 1975, sample FD102, slide a, K36/4.
14. *Pareodinia* spp., Deflandre, 1947d, sample FD102, slide b, W42/2.15.
15. *Pareodinia ceratophora*, Deflandre, 1947d, sample FD18, slide a, M37/3.
16. *Pareodinia ceratophora*, Deflandre, 1947d, sample FD18, slide a, O31/4.



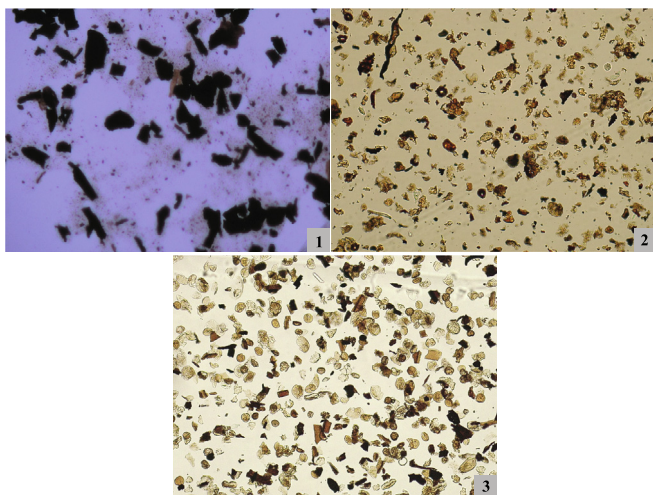


Plate XII. Photo micrographs of Palynofacies from the upper Bajocian to Lower Bathonian in the Al Feddane (FD) section, Skoura syncline, Middle Atlas, Morocco.

1. Palynofacies (FD47) of the 1st category (it corresponds to the fifty-one samples represented by white bars in the section FD). It is composed of 100% degraded, carbonaceous and black phytoclasts (MOx, inertinite).
2. Palynofacies (FD88), of the 2nd category. It is composed of Phytoclasts (Mob), amorphous organic matter (Moa) and palynomorphs.
3. Palynofacies (FD100), of the 2nd category, dinoflagellate cysts are dominant on the Mob and Moa.

Tubotuberella dangardii (Sarjeant, 1968) Stover and Evitt, 1978.

Valensiella ovulum (Deflandre, 1947d) Eisenack, 1963a, Emend: Courtinat, 1989.

Valensiella vermiculata (Gocht, 1970b).

Wanaea acollaris (Dodekova, 1975) Emend: Riding and Helby, 2001b.

Willeidinium spp. (Feist-Burkhardt, 1995a).

A.2. Spores and pollen grains

Alisporites robustus Nilsson, 1958.

Araucariacites australis Cookson, 1947.

Callialasporites dampieri (Balme) Sukh Dev 1961.

Callialasporites segmentatus Srivastava, 1963.

Callialasporites turbatus Schulz, 1967.

Plate XI. Photo micrographs of Palynomorphs from the upper Bajocian to Lower Bathonian in the Al Feddane (FD) section, Skoura syncline, Middle Atlas, Morocco. Each specimen identified by sample, slide number and England finder coordinates. Scale bar in Figure represent 20 µm.

1. *Cyathidites minor*, Couper, 1953, Sample FD100, Slide a, K31.
2. *Gleicheniidites senonicus* Ross, 1949, Sample FD100, Slide a, N23/4.
3. *Ischyosporites variegatus*, Couper 1958, Sample FD100, Slide a. Q32/1.
4. *Lycopodiumsporites austroclavatidites*, Couper, 1958, Sample FD100, Slide a. S33/1.
5. *Araucariacites australis*, Cookson, 147, Sample FD100, Slide a. R17.
- 6–7. *Leptolepidites* sp., Couper, 1953, Sample FD100, Slide a. M13.
8. *Leptolepidites* sp., Couper, 1953, Sample FD78, Slide a. G41/4.
9. *Callialasporites dampieri*, (Balme) Sukh Dev 1961, Sample FD101, Slide b. R26/4.
10. *Callialasporites segmentatus*, Srivastava, 1963, Sample FD64, Slide a. H16.
11. *Callialasporites turbatus*, (Balme) Schulz, 1967, Sample FD106, Slide a. J50.
12. *Vitreisporites pallidus*, Nilsson, 1958, Sample FD7, Slide a. N39.
13. *Alisporites robustus*, Nilsson, 1958, Sample FD105, Slide a. G34.
14. *Classopolis* spp., Pflug, 1953, Sample FD100, Slide a. K25.
15. *Dasycladaceae Dobunniella*, Elliott, 1975, Sample FD14; FD101.
16. *Tasmanites* (Prasinophytes), Sample FD34, Slide b. Q13/3.
17. *Skolokodonts*, Sample FD100, Slide a. M29/1.
18. Foraminiferal test lining, Sample FD5, Slide a. N54.
19. *Dasycladaceae*, transversal reconstruction of the thallus, Sample FD14; Slide a.V29; H33.
20. *Micrhystridium* spp., Sample FD100–102, Slide a.
21. *Micrhystridium lymensis*, Wall, 1965, Sample FD100, Slide a.
- 22–23. *Acritarchs*, Sample FD102, Slide a.
24. *Crassospaera*, (Prasinophyte), Cookson and Manum, 1960, Sample FD100, Slide a. M12. (*100).
25. *Crassospaera*, (Prasinophyte), Cookson and Manum, 1960, Sample FD100, Slide a. R24.

Classopolis spp. Pflug, 1953.

Cyathidites spp. Couper 1958.

Gleicheniidites senonicus Ross, 1949.

Ischyosporites variegatus Couper 1958.

Leptolepidites sp. Couper, 1953.

Lycopodiumsporites austroclavatidites Couper, 1958.

Vitreisporites pallidus Nilsson, 1958.

References

- Alméras, Y., Fauré, P., Elmi, S., Enay, R., Mangold, C., 2007. Zonation des brachiopodes du Jurassique moyen sur la marge sud de la Téthys occidentale (Maroc, Algérie occidentale): Comparaison avec la marge nord-téthysienne française. *Geobios* 40 (1), 1–19.
- Bailey, D.A., 1987. *Durotrigia daveyi* gen. et sp. nov., an Early Bajocian dinocyst with a variable precingular archaeopyle. *J. Micropalaeontol.* 6, 89–96.
- Batten, D.J., 1999. Palynofacies analysis. In: Jones, T.P., Rowe, N.P. (Eds.), *Fossil plants and Spores: Modern Techniques*. Geol. Soc, London, pp. 194–198.
- Batten, D.J., Dutta, R.J., 1997. Ultrastructure of exine of gymnospermous pollen grains from Jurassic and basal Cretaceous deposits in Northwest Europe and implications for botanical relationships. *Rev. Palaeob. Palynol.* 99, 25–54.
- Batten, D.J., Koppelman, E.B., 1996. Chapter 20D. Biostratigraphic significance of uppermost Triassic and Jurassic miospores in Northwest Europe. In: Jansonius, J., McGregor, D.C. (Eds.), *Palynology: Principles and Applications*. Am. Assoc. Stratigr. Palynol. Foundvol. 2, pp. 795–806.
- Batten, D.J., Lister, J.K., 1988. Evidence of freshwater dinoflagellates and other algae in the English Wealden (Early Cretaceous). *Cretac. Res.* 9 (2), 171–179.
- Benshili, K., 1989. *Lias-Dogger du Moyen Atlas plissé (Maroc)*, sédimentologie, biostratigraphie et évolution paléogéographique. *Travaux et Documents des Laboratoires de Géologie de Lyon* 106 (1), 3–285.
- Carvalho, M.A., Bengtson, P., Lana, C.C., 2016. Late Aptian (Cretaceous) paleoceanography of the South Atlantic Ocean inferred from dinocyst communities of the Sergipe Basin, Brazil. *Paleoceanography* 31, 2–26.
- Charrière, A., 1989. Carte géologique au 1/100 000. Feuille de Sefrou. Notes et Mém. Serv. géol. Maroc, p. 354.
- Charrière, A., 1990. Héritage hercynien et évolution géodynamique alpine d'une chaîne intracontinentale : le Moyen Atlas au SE de Fès (Maroc). (Thèse d'État) Univ. Toulouse III, France.
- Charrière, A., 1992. Discontinuités entre les « Couches rouges » du Jurassique moyen et du Crétacé inférieur dans le Moyen-Atlas (Maroc). *C.R. Acad. Sci. Paris, Ser. II* 315, 1389–1393.
- Charrière, A., Dépêche, F., Feist, M., Grambast-Fessard, N., Jaffrezo, M., Peybernès, B., Ramalho, M., 1994. Microfaunes, microflores et paléoenvironnements successifs dans la Formation d'El Mers (Bathonien-? Callovien) du synclinale de Skoura (Moyen-Atlas, Maroc). *Geobios* 27 (2), 157–174.
- Charrière, A., Haddoumi, H., 2016. Dater les couches rouges continentales pour définir la géodynamique Atlasique. *Géologues* 194, 29–32.
- Choubert, G., 1956. Carte géologique du Maroc, feuille de Rabat au 1/500000. Notes Mem. Serv. Geol. Maroc, p. 70.
- Choubert, G., Faure-Muret, A., 1967. Le Jurassique de la région d'El Mers-Skoura. Notes Mem. Serv. Geol. Maroc. 200, pp. 1–32.
- Colo, G., 1961. Contribution à l'étude du Jurassique du Moyen Atlas septentrional. Notes Mem. Serv. Geol. Maroc, p. 139.

- Combaz, A., 1964. Les palynofacies. Rev. Micropaleontol. 7, 205–218.
- Conway, B.H., 1990. Paleozoic-Mesozoic palynology of Israel. II. Palynostratigraphy of the Jurassic succession in the subsurface of Israel. Isr. Geol. Surv. Bull. 82, 1–39.
- Correia, V.F., Riding, J.B., Duarte, L.V., Fernandes, P., Pereira, Z., 2018. The Early Jurassic palynostratigraphy of the Lusitanian Basin, western Portugal. Geobios 51 (6), 537–557.
- Dale, B., 1983. Dinoflagellate resting cysts: benthic plankton. In: Fryxell, G.A. (Ed.), Survival Strategies of the Algae. Cambridge University Press, pp. 69–136.
- Davey, R.J., 1970. Non-calcareous microplankton from the Cenomanian of England, northern France and North America, part II. Bull. Brit. Mus. (Nat. Hist.). Geol. 18, 333–397.
- Dresnay, R., 1963. Données stratigraphiques complémentaires sur le Jurassique moyen des synclinaux d'El Mers et de Skoura (Moyen-Atlas, Maroc). Bull. Soc. Geol. France 7 (6), 883–900.
- Dresnay, R., 1969. Discussions stratigraphiques sur les conditions de gisements de bois fossiles mésozoïques du Maroc étudiés par. In: Attims, M.Y., Cremier, F., Gazeau, F. (Eds.), Bois fossiles mésozoïques du Maroc, 210. Notes & Mem. Serv. Geol. Maroc, pp. 121–178.
- Dresnay, R., 1975. Données topographiques, stratigraphiques et paléontologiques concernant une ammonite citée dans la Formation d'El Mers (Moyen-Atlas, Maroc) et leurs conséquences sur l'âge attribué à cette formation. Bull. Soc. Géol. France (7), XVII 6, 1144–1146.
- Duée, G., Hervouet, T., Laville, E., Luca, P., Robillard, D., 1977. L'accident nord moyen-atlasique dans la région de Boulemane (Maroc): une zone de coulistement synsédimentaire. Ann. Soc. Géol. Nord, Lille XCVIII, pp. 145–162.
- El Beialy, S.Y., Ibrahim, M.I., 1997. Callovian-Oxfordian (Middle-Upper Jurassic) microplankton and miospores from the Masajid Formation, WX1 boreholes, El Maghara area, North Sinai, Egypt: biostratigraphy and palaeoenvironmental interpretation. Neues Jb. Geol. Paläontol. Abh. 204, 379–398.
- Fauconnier, D., 1995. Jurassic palynology from a borehole in the Champagne area, France—correlation of the lower Callovian-middle Oxfordian using sequence stratigraphy. Rev. Palaeobot. Palynol. 87, 15–26.
- Fedan, B., 1993. Évolution géodynamique d'un bassin intraplaque sur décrochements: Le Moyen Atlas (Maroc) durant le Méso-Cénozoïque (Thèse Doctorat État), 18. Trav. Instit. Sci. Rabat (1989), sér. Géologie-Géographie physique.
- Fedan, B., Laville, E., El Mezgueldi, A., 1989. Le bassin jurassique du Moyen Atlas (Maroc): un exemple de bassin sur relais de décrochements. Bull. Soc. Geol. France 6, 1123–1136.
- Feist-Burkhardt, S., 1990. Dinoflagellate cyst assemblages of the Hauses coreholes (Aalenian to Early Bajocian), Southwest Germany. Elf-Aquitaine, Pau, France. Bulletin des centres de recherches exploration - Production Elf-Aquitaine 14/2, 611–633.
- Feist-Burkhardt, S., Gotz, A.E., 2016. Ultra-high-resolution palynostratigraphy of the Early Bajocian Sauzei and Humphriesian zones (Middle Jurassic) from outcrop sections in the Upper Rhine Area, Southwest Germany. Stratigr. Timescales 1, 325–392.
- Feist-Burkhardt, S., Monteil, E., 1997. Dinoflagellate cysts from the Bajocian stratotype (Calvados, Normandy, western France). Bulletin des centres de recherches exploration Production Elf-Aquitaine 21, 31–105.
- Feist-Burkhardt, S., Monteil, E., 2001. Gonyaulacean dinoflagellate cysts with multiplate precingular archaeopyle. Neues Jah. Geol. Paläontol. –Abh. 219 (1/2), 33–81.
- Feist-Burkhardt, S., Wille, W., 1992. Jurassic palynology in southwest Germany. State of the art - 8th International Palynological Congress, Aix-en-Provence, 13–16th Sept. 1992. Cah. Micropaléontol. 105, 141–156.
- Fensome, R.A., Riding, J.B., Taylor, F.J.R., 1996. Dinoflagellates. In: Jansonius, J., McGregor, D.C. (Eds.), Palynology: Principles and Applications. American Association of Stratigraphic Palynologists Foundation, Dallas, Texas, pp. 107–169.
- Fensome, R.A., Taylor, F.J.R., Norris, G., Sarjeant, W.A.S., Wharton, D.I., Williams, G.L., 1993. A classification of fossil and living dinoflagellates. Micropaleontology Press Special Paper 7, 351.
- Fenton, J.P.G., 1981. Taxonomic revision of selected dinoflagellate cysts from the late Bajocian (Middle Jurassic) of northwest Germany. Rev. Palaeobot. Palynol. 31, 249–260.
- Fenton, J.P.G., Riding, J.B., Wyatt, R.J., 1994. Palynostratigraphy of the Middle Jurassic 'White Sands' of Central England. Proc. Geol. Assoc. 105, 225–230.
- Fenton, J.P.G., Riding, J.B., Wyatt, R.J., 1995. Palynostratigraphy of the Middle Jurassic "White Sands" of Central England, by Fenton, Riding and Wyatt (1994): Reply. Proc. Geol. Assoc. 106, 306–308.
- Frizon de Lamotte, D., Zizi, M., Missenard, Y., Hafid, M., El Azzouzi, M., Maury, R.C., Charrère, A., Taki, Z., Benammi, M., Michard, A., 2008. The Atlas system. In: Michard, A., Saddiqi, O., Chalouan, A., Frizon de Lamotte, D. (Eds.), Continental Evolution: The Geology of Morocco. Lect. Notes Earth Sci 116, pp. 133–202.
- Ghasemi-Nejad, E., Sabbaghiyan, H., Mosaddegh, H., 2012. Palaeobiogeographic implications of Late Bajocian-Late Callovian (Middle Jurassic) dinoflagellate cysts from the Central Alborz Mountains, northern Iran. J. Asian Earth Sci. 43, 1–10.
- Goodman, David K., 1979. Dinoflagellate "communities": from the lower Eocene Nanjemoy formation of Maryland, U.S.A. Palynology 3 (1), 169–190.
- Gorin, E.G., Steffen, D., 1991. Organic facies as atool for recording eustatic variations in marine fine-grained carbonates—example of the Berriasian stratotype at Berrias (Ardèche, SE France). Palaeogeogr. Palaeoclimatol. Palaeoecol. 85, 303–320.
- Habib, D., Miller, J.A., 1989. Dinoflagellate species and organic fades evidence of marine transgression and regression in the Atlantic Coastal Plain. Palaeogeogr. Palaeoclimatol. Palaeoecol. 74, 23–47.
- Habib, D., Moshkovitz, S., Kramer, C., 1992. Dinoflagellate and calcareous nannofossil response to sea-level change in Cretaceous-Tertiary boundary sections. Geology 20 (2), 165–168.
- Hallam, A., 2001. A review of the broad pattern of Jurassic sea-level changes and their possible causes in the light of current knowledge. Palaeogeogr. Palaeoclimatol. Palaeoecol. 167 (1–2), 23–37.
- Haq, B.U., 2018. Jurassic sea-level variations: a reappraisal. Geol. Soc. Am. Today 28 (1), 4–10.
- Hergreen, G.F.W., De Boer, K.F., 1984. Palynology of the Upper Jurassic, Central Graben, Scruff, and Delfland Groups in the Dutch Part of the North Sea Continental Shelf. International Symposium on Jurassic Stratigraphy 3, 696–714.
- Hssaida, T., 1990. Étude palynologique, kystes de dinoflagellés du Jurassique (Bathonien-Callovien-Oxfordien) du bassin de Guercif, Maroc. Thèse Université Rennesp. 215 (inédit).
- Hssaida, T., 1995. Étude palynologique (kyste de dinoflagellés, palynofaciès) de gisements Bathonien supérieur à Oxfordien inférieur de Normandie et Cévennes (France), de Guercif (Maroc). Biostratigraphie, Paleo-environnement et Paleo-biogéographie. Thèse de Doctorat ès Sciences Rabatp. 255 (inédit).
- Hssaida, T., Benzaggagh, M., Riding, J.B., Huault, V., Essamoud, R., Mouflih, M., Jaydawi, S., Chakir, S., Nahim, M., 2017. Répartition stratigraphique et biozones des kystes de dinoflagellés au passage Jurassique moyen-Jurassique supérieur (Bathonien supérieur-Oxfordien inférieur) dans le Bassin de Guercif, Maroc nord-oriental. Ann. Paléontol. 103 (3), 197–215.
- Hssaida, T., Morzadec-Kerfourn, M.T., 1993. Kystes de dinoflagellés et palynofaciès: indicateurs des variations bathymétriques dans le bassin de Guercif (Maroc) au Jurassique (Bathonien terminal-Oxfordien basal). Rev. Palaeobot. Palynol. 77, 97–106.
- Ibrahim, M., Aboul Ela, N.M., Kholeif, S.E., 2001. Palynostratigraphy of Jurassic to Lower Cretaceous sequences from the Eastern Desert of Egypt. J. Afr. Earth Sci. 32 (2), 269–297.
- Jan du Chene, R.E., et al., 1985. Taxonomic problems concerning the revision of "Gonyaulax" cornigera Valensi 1953, a fossil dinoflagellate cyst. [Problèmes taxonomiques liés la révision de l'espèce "Gonyaulax" cornigera Valensi, 1953, kyste fossile de dinoflagelle]. Rev. Micropaleontol. 28 (2), 109–124.
- Jaydawi, S., Hssaida, T., Benbouziane, A., Mouflih, M., Alami, Chakor, 2016. Datation par les kystes de dinoflagellés des formations jurassiennes (Callovien-Kimméridgien) du bassin d'Essaouira (Marge atlantique marocaine). Bulletin de l'Institut Scientifique, Rabat, Section Sciences de la Terre 38, 127–148.
- Lapparent, A.F., 1955. Etude paléontologique des vertébrés du Jurassique d'El Mers (Moyen Atlas). Notes Mém. Serv. Géol. Maroc. 124, pp. 1–36.
- Laville, E., Fedan, B., 1989. Le système atlasicus marocain au jurassique : évolution structurale et cadre géodynamique. Sci. Géol. Mém. Strasbourg 84, 3–28.
- Leckie, D., Singh, C., 1991. Estuarine deposits of the Albian Paddy Member (Peace River Formation) and lowermost Shaftesbury Formation, Alberta, Canada. J. Sediment. Res. 61, 825–849.
- Leckie, D.A., Singh, C., Bloch, J., Wilson, M., Wall, J., 1992. An anoxic event at the Albian Cenomanian boundary: The Fish Scale Marker Bed, northern Alberta. Palaeogeogr. Palaeoclimatol. Palaeoecol. 92, 139–166.
- Lister, J., Batten, D., 1988. Stratigraphic and palaeoenvironmental distribution of early Cretaceous dinoflagellate cysts in the Hurlands Farm borehole, West Sussex, England. Palaeontogr. Abt. B 210, 9–89.
- MacArthur, R.H., Wilson, E.O., 1967. The Theory of Island Biogeography. Princeton Univ. Press, Princeton, NJ, p. 203.
- Mafi, A., Ghasemi-Nejad, E., Ashouri, A., Vahidi-Nia, M., 2013. Dinoflagellate cysts from the Upper Bajocian-Lower Oxfordian of the Dalichai Formation in Binalud Mountains (NE Iran): their biostratigraphical and biogeographical significance. Arab. J. Geosci. 7, 3683–3692.
- Mantle, D.J., Riding, J.B., 2012. Palynology of the Middle Jurassic (Bajocian-Bathonian) *Wana verrucosa* dinoflagellate cyst zone of the North West Shelf of Australia. Rev. Palaeobot. Palynol. 180, 41–78.
- Martin, J., 1973. Carte géomorphologique du Moyen Atlas central au 1/100000. Notes Mém. Serv. géol. Maroc 258, 5 feuilles.
- Martin, J., 1981. Le Moyen Atlas Central, étude géomorphologique. Notes Mém. Serv. géol. Maroc 258 bis.
- Melia, M.B., 1984. The distribution and relationship between palynomorphs in aerosols and deep-sea sediments off the coast of northwest Africa. Mar. Geol. 58, 345–371.
- Mongin, D., 1963. Les Mollusques du Bathonien-Callovien saumâtre du Moyen-Atlas (Maroc). C. R. Acad. Sci. 256 (21), 4469–4470.
- Mongin, D., 1967. Les mollusques du Bathonien saumâtre du moyen Atlas. Notes et Mémoires du Service Géologique du Maroc. 200, pp. 37–92.
- Moyné, S., Neige, P., 2007. The space-time relationship of taxonomic diversity and morphological disparity in the Middle Jurassic ammonite radiation. Palaeogeogr. Palaeoclimatol. Palaeoecol. 248, 82–95.
- Mutterlose, J., Harding, I., 1987. Phytoplankton from the anoxic sediments of the Barremian (lower Cretaceous) of north-West Germany. Abh. Geo. Bundes. 39, 177–215.
- Oukassou, M., 2018. Mise en évidence ichnologique des Xiphosures du Jurassique au Maroc : Contexte géologique, paléoenvironnemental et paléobiogéographique. Thèse d'Habilitation UniversitaireUniversité Hassan II de Casablanca, Maroc, p. 82.
- Oukassou, M., Boumir, Kh., Benshili, Kh., Ouahrache, D., Lagnaoui, A., Charrère, A., 2019. The Tichoukt Massif: a Geotouristic Play in the Folded Middle Atlas (Morocco). Geohéritage 11, 371–379.
- Oukassou, M., Charrière, A., Lagnaoui, A., Gibb, S., Michard, A., Saddiqi, O., 2016. First occurrence of the ichnogenus *Selenichnites* from the Middle Jurassic Strata of the Skoura Syncline (Middle Atlas, Morocco); palaeoecological and palaeoenvironmental context. Comptes Rendus Palevol. 15, 461–471.
- Pocklington, R., Leonard, J.D., 1979. Terrigenous Organic Matter in Sediments of the St. Lawrence Estuary and the Saguenay Fjord. J. Fish. Res. Board Can. 36 (10), 1250–1255.
- Poulsen, N.E., 1998. Upper Bajocian to Callovian, (Jurassic), dinoflagellate cysts from central Poland. Acta Geol. Pol. 48 (3), 237–245.
- Poulsen, N.E., Riding, J.B., 2003. The Jurassic dinoflagellate cyst zonation of Subboreal Northwest Europe. Geological Survey of Denmark and Greenland Bulletin 1, 115–144.

- Rhrrib, J., 1997. Die Störungszonen des Mittleren Atlas (Zentralmarokko) Strukturelle Entwicklung in einem intrakontinentalen Gebirge. Berliner Geowiss. Abh. A 194, 1–221.
- Riding, J.B., 1983. The palynology of the Aalenian (Middle Jurassic) sediments of Jackdaw Quarry, Gloucestershire, England. Mercian Geol. 9, 111–120.
- Riding, J.B., 1984. Dinoflagellate cyst range top biostratigraphy of the uppermost Triassic to lowermost Cretaceous of northwest Europe. Palynology 8, 195–210.
- Riding, J.B., 1994. Appendix 2; Palynofloras of the Oxford Clay Formation. In: Martil, D., Taylor, M.A., Duff, K., Riding, J.B., Bown, P., (Eds.), The Trophic Structure of the biota of the Peterborough Member, Oxford Clay Formation (Jurassic), U.K. J. Geol. Soc. 151 (1), 190–194.
- Riding, J.B., Mantle, D.J., Backhouse, J., 2010. A review of the chronostratigraphical ages of Middle Triassic to Late Jurassic dinoflagellate cyst biozones of the North West Shelf of Australia. Rev. Palaeobot. Palynol. 162, 543–575.
- Riding, J.B., Penn, I.E., Woollam, R., 1985. Dinoflagellate cysts from the type area of the Bathonian stage (middle Jurassic; Southwest England). Rev. Palaeobot. Palynol. 45 (1–2), 149–151 155–169.
- Riding, J.B., Thomas, J.E.R., 1992. Dinoflagellate cysts of the Jurassic System. In: Powell, A.J. (Ed.), A Stratigraphic Index of Dinoflagellate cysts. Chapman and Hall, London, pp. 7–98.
- Riding, J.B., Thomas, J.E.R., 1997. Marine palynomorphs from the Staffin Bay and Staffin Shale formations (Middle–Upper Jurassic) of the Trotternish Peninsula, NW Skye. Scott. J. Geol. 33, 59–74.
- Riding, J.B., Walton, W., Shaw, D., 1991. Toarcian to Bathonian (Jurassic) palynology of the Inner Hebrides, northwest Scotland. Palynology 15, 115–179.
- Rousselle, L., 1963. A propos de *Flabellothyris oranensis* (Flamand), brachiopode du Dogger moyen. Bull. Soc. Géol. France 1, 41–46.
- Rousselle, L., 1965. Rhynchonellidae, Terebratulidae et Zeilleriidae du Dogger marocain (Moyen-Atlas septentrional, Hauts-Plateaux Haut-Atlas). Travaux de l'Institut scientifique chérifien, Série géologie et géographie physique 13, 5–168.
- Rousselle, L., 1966. Remarques sur la répartition verticale et l'écologie de *Burmimirynchia ? termierae*, seul Brachiopode connu de la formation supérieure des synclinaux de Skoura et d'El Mers Dogger du Moyen-Atlas sep. Compte Rendu Sommaire des Séances de la Société Géologique de France 9, 346–347.
- Scheele, J., 1994. Vom frühmesozoischen Riftgraben zum intrakontinentalen Gebirge: Konvergente Blattverschiebungstektonik im zentralen Mittleren Atlas (Marokko). Berl. Geowiss. Abh. A 160–173.
- Smelror, M., 1993. Biogeography of Bathonian to Oxfordian (Jurassic) dinoflagellates: Arctic, northwest Europe and Circum-Mediterranean. Palaeogeogr. Palaeoclimatol. Palaeoecol. 102 (1), 121–160.
- Tahoun, S.S., Deaf, A.S., Mansour, A., 2017. Palynological, palaeoenvironmental and sequence stratigraphical analyses of a Turonian-Coniacian sequence, Beni Suef Basin, Eastern Desert, Egypt: implication of *Pediastrum* rhythmic signature. Mar. Pet. Geol. 88, 871–887.
- Termier, H., 1936. Etude géologique sur le Maroc central et le Moyen Atlas septentrional. Notes et Mémoires du Service Géologique du Maroc, Rabat, 33, II, pp. 890–982.
- Termier, H., Termier, G., 1967. L'estran sablo-vaseux du Bathonien pendant l'exondation de la série d'El Mers (Moyen Atlas marocain). Comptes rendus de l'Académie des Sciences, Série D 265 (14), 947–949.
- Tyson, R.V., 1993. Palynofacies analysis. In: Tyson, R.V., Jenkins, D.G. (Eds.), Applied Micropalaeontology. Kluwer Academic Publishers, Dordrecht, pp. 153–191.
- Tyson, R.V., 1995. Sedimentary Organic Matter: Organic Facies and Palynofacies. Chapman and Hall, London, p. 615.
- Versteegh, G.J.M., 1994. Recognition of cyclic and non-cyclic environmental changes in the Mediterranean Pliocene: a palynological approach. Mar. Micropaleontol. 23, 147–183.
- Wall, D., Dale, B., Lohmann, G.P., Smith, W.K., 1977. The environment and climatic distribution of dinoflagellate cysts in modern marine sediments from regions in the North & South Atlantic Oceans and adjacent seas. Mar. Micropal. 2, 121–200.
- Whitaker, M.F., Giles, M.R., Cannon, S.J.C., 1992. Palynological review of the Brent Group, UK sector, North Sea. Geol. Soc. Lond. Spec. Publ. 61 (1), 169–202.
- Wiggan, N.J., Riding, J.B., Fensome, R.A., Mattioli, E., 2018. The Bajocian (Middle Jurassic): a key interval in the early Mesozoic phytoplankton radiation. Earth Sci. Rev. 180, 126–146.
- Wiggan, N.J., Riding, J.B., Franz, M., 2017. Resolving the Middle Jurassic dinoflagellate radiation: the palynology of the Bajocian of Swabia, southwest Germany. Rev. Palaeobot. Palynol. 238, 55–87.
- Williams, G.L., Bujak, J.P., 1985. Mesozoic and Cenozoic dinoflagellates. In: Bolli, H.M., Saunders, J.B., Perch-Nielsen, K. (Eds.), Plankton Stratigraphy. Cambridge University Press, Cambridge, pp. 847–964.
- Williams, G.L., Stover, I.E., Kidson, E.J., 1993. Morphology and stratigraphic ranger of selected Mesozoic-Cenozoic dinoflagellate taxa in the northern Hemisphere. Geological Survey of Canada Paper 92 (10), 1–137.
- Woollam, R., Riding, J.B., 1983. Dinoflagellate cyst zonation of the English Jurassic. Institute of Geological Sciences, Report 83/2, 1–41.